

Subspace Thresholding Pursuit: A Reconstruction Algorithm for Compressed Sensing

Chao-Bing Song, Shu-Tao Xia

Abstract

We propose a new iterative greedy algorithm for reconstructions of sparse signals with or without noisy perturbations in compressed sensing (CS). The proposed algorithm, called *subspace thresholding pursuit* (STP) in this paper, is a simple combination of subspace pursuit and iterative hard thresholding which are two important greedy reconstruction algorithms. In view of theoretical guarantee, we show that STP with parameter $\mu = 1$ can reconstruct arbitrary signals with bounded mean square error under sparsity defect and measurement error if the measurement matrix satisfies the *restricted isometry property* with $\delta_{3s} < 0.5340$. Particularly, if $\delta_{3s} < 0.5340$, it can reconstruct any s -sparse signals perfectly in noiseless environment. In view of empirical performance, STP with proper μ can outperform other state-of-the-art reconstruction algorithms greatly when reconstructing Gaussian signals. Furthermore, when reconstructing constant amplitude signals with random signs (CARS signals), unlike other known iterative greedy algorithms which usually perform significantly worse than the well-known ℓ_1 minimization, the proposed STP algorithm with proper μ can outperform the ℓ_1 minimization in most practical cases. In addition, we propose a simple but effective method to solve the overfitting problem when the undersampling ratio is large. Finally, we generalize the idea of STP to other state-of-the-art algorithms and the modified algorithms have better empirical performance than the original ones.

Index Terms

Compressed sensing, restricted isometry constants, reconstruction algorithms, subspace thresholding pursuit, sparse recovery

I. INTRODUCTION

As a new paradigm for signals sampling, compressed sensing (CS) [1]–[3] has attracted a lot of attention in recent years. Consider an s -sparse signal $\mathbf{x} = (x_1, x_2, \dots, x_N) \in \mathbb{R}^N$ which has at most s nonzero entries. Let $\Phi \in \mathbb{R}^{m \times N}$ be a measurement matrix with $m \ll N$ and $\mathbf{y} = \Phi \mathbf{x}$ be a measurement vector. CS deals with recovering the original signal \mathbf{x} from the measurement vector \mathbf{y} by finding the sparsest solution to the underdetermined linear system $\mathbf{y} = \Phi \mathbf{x}$, i.e., solving the following ℓ_0 minimization problem:

$$\min \|\mathbf{x}\|_0 \quad s.t. \quad \Phi \mathbf{x} = \mathbf{y}, \quad (1)$$

where $\|\mathbf{x}\|_0 := |\{i : x_i \neq 0\}|$ denotes the ℓ_0 -norm of \mathbf{x} . In addition, let $\tau = \frac{m}{N}$ denote the undersampling ratio. From [4], we know that the maximal sparsity of the signals that ℓ_0 minimization can reconstruct uniformly is upper bound by $\lceil m/2 \rceil$. Unfortunately, as a typical combinatorial optimization problem, this

This research is supported in part by the Major State Basic Research Development Program of China (973 Program, 2012CB315803), the National Natural Science Foundation of China (61371078), and the Research Fund for the Doctoral Program of Higher Education of China (20100002110033).

All the authors are with the Graduate School at ShenZhen, Tsinghua University, Shenzhen, Guangdong 518055, P.R. China (e-mail: scb12@mails.tsinghua.edu.cn, xiazt@sz.tsinghua.edu.cn).

optimal recovery algorithm is NP-hard [2]. One popular strategy is to relax the ℓ_0 minimization problem to a ℓ_1 *minimization* problem:

$$\min \|\mathbf{x}\|_1 \quad s.t. \quad \Phi \mathbf{x} = \mathbf{y}. \quad (2)$$

Due to the convexity of ℓ_1 minimization, we can solve it in polynomial time [2] by linear programming techniques. But the computational complexity $\mathcal{O}(N^3)$ of linear programming is still too high for practical use.

Based on special combinatorial structure and decoding algorithms from coding theory, some extremely fast sublinear algorithms have been proposed, such as Expander Recovery Algorithm in [5] and the algorithm based on Belief Propagation in [6]. But they depend on the structure of measurement matrix deeply, which leads to the need for some unusual sample which may not be easy to acquire in practice.

Compared with ℓ_1 minimization, it is the family of iterative greedy algorithms that can reduce the computational complexity greatly, possess the similar empirical performance and provide the reconstruction guarantee described by a common property of measurement matrix called *restricted isometry property* (RIP). As powerful alternatives to ℓ_1 minimization, a lot of iterative greedy algorithms have been proposed and analyzed. According to the way of greedily selecting the columns of measurement matrix, we can divide current iterative greedy algorithms into two kinds: the algorithms of the one kind are variants of orthogonal matching pursuit (OMP) [7] called OMP-like algorithms, such as OMP itself, regularized OMP [8], compressive sampling matching pursuit (CoSaMP) [9], subspace pursuit (SP) [10], generalized OMP (GOMP) [11] or orthogonal multi matching pursuit (OMMP) [12], sparsity adaptive matching pursuit (SAMP) [13], forward backward pursuit (FBP) [14], and that of the other kind variants of iterative hard thresholding (IHT) [15] called IHT-like algorithms, such as IHT itself, gradient descent with sparsification (GDS) [16], hard thresholding pursuit (HTP) [17], normalized iterative hard thresholding (NIHT) [18]. In all of these algorithms, the representatives may be SP, CoSaMP, HTP and NIHT. They have provable theoretical guarantees comparable to that of ℓ_1 minimization and good empirical performance to reconstruct constant amplitude signals with random signs (CARS signals) when compared with other iterative greedy algorithms.

In view of theoretical guarantee, Table I shows the sufficient conditions with respect to *restricted isometry constants* (RICs) δ with some orders for OMP, IHT and the four representatives above to perfectly reconstruct s -sparse signals.

Table I
SUFFICIENT CONDITIONS OF ITERATIVE GREEDY ALGORITHMS TO PERFECTLY RECONSTRUCT S-SPARSE SIGNALS

OMP [19], [20]	SP [21]	CoSaMP [21]	IHT [17, Theorem 3.7]	HTP [17]	NIHT [22]
$\delta_{s+1} < \frac{1}{\sqrt{s+1}}$	$\delta_{3s} < 0.4859$	$\delta_{4s} < 0.5$	$\delta_{3s} < \frac{1}{\sqrt{3}} \approx 0.5773$	$\delta_{3s} < \frac{1}{\sqrt{3}} \approx 0.5773$	$\delta_{3s} < 0.2$

In view of empirical performance, all iterative greedy algorithms have good performance when reconstructing Gaussian signals, while relatively bad performance when reconstructing the CARS signals. From [23], Maleki and Donoho show that CARS signals may be the most difficult kind of signals that iterative greedy algorithms can reconstruct. It is noteworthy that although a lot of iterative greedy algorithms can outperform ℓ_1 minimization when reconstructing Gaussian signals, to the best of our knowledge, there is no existing iterative greedy algorithm that can outperform ℓ_1 minimization when reconstructing CARS signals.

In this paper, our main contribution is a new algorithm, termed *subspace thresholding pursuit* (STP). By finding that the idea of IHT-like algorithms can improve the approximation effect of OMP-like algorithms efficiently, we combine the steps of SP and IHT in one iteration, thus acquiring a better empirical performance. STP is convenient to be analyzed theoretically, since the theoretical guarantees of SP and IHT are established well and STP is only a simple combination of them. In our analysis, STP with parameter $\mu \geq 0$ can reconstruct s -sparse signals perfectly in noiseless environment when the RIC condition is comparable to that of ℓ_1 minimization, i.e., it is upper bound by a positive constant. Particularly, when $\mu = 1$, STP can guarantee the exact s -sparse recovery if $\delta_{3s} < 0.5340$, which is better than the theoretical guarantee of SP, but a little weaker than that of IHT. The theoretical results also apply to almost sparse signals and corrupted measurements. Compared with theoretical guarantee, empirical performance is a more important aspect that makes STP different. When reconstructing Gaussian signals, STP with proper μ can outperform other state-of-the-arts reconstruction algorithms greatly. If the original signal is sampled by a relatively practical undersampling ratio, the STP's empirical performance measured by *critical sparsity* can be up to twice of that of ℓ_1 minimization. When reconstructing CARS signals, STP can outperform ℓ_1 minimization under a relatively practical undersampling ratio. To the best of our knowledge, it is the first iterative greedy algorithm that can break the bottleneck, i.e., outperform the reconstruction capability of ℓ_1 minimization in CARS signal case, thus showing a good application prospect. In addition, we propose a simple but effective method to solve “the overfitting problem” of STP, thus making the reconstruction capability of STP exceed the limitation $\lceil m/2 \rceil$ in Gaussian signal

case if the undersampling ratio is large. Furthermore we generalize the idea of STP to other state-of-the-art iterative greedy algorithms and the resulting algorithms show better empirical performance than the original ones.

The remainder of the paper is organized as follows. Section II introduces the basic notations, definitions and lemmas. Section III gives the algorithm description and theoretical analysis. Section IV gives the performance simulations and analyses. Section V gives some extended study. Finally, we conclude the paper in Section VI.

II. PRILIMINARIES

Let $\mathbf{x} = (x_1, x_2, \dots, x_N) \in \mathbb{R}^N$. Let $T \subseteq \{1, 2, \dots, N\}$, and $|T|$ and \bar{T} respectively denote the cardinality and complement of T . Let $\mathbf{x}_T \in \mathbb{R}^N$ denote the vector obtained from \mathbf{x} by keeping the $|T|$ entries in T and setting all other entries to zero. Let $\text{supp}(\mathbf{x})$ denote the supports of \mathbf{x} or the set of indices of nonzero entries in \mathbf{x} . Note that \mathbf{x} is s -sparse if and only if $|\text{supp}(\mathbf{x})| \leq s$. For a matrix $\Phi \in \mathbb{R}^{m \times N}$, let Φ^* denote the (conjugate) transpose of Φ and Φ_T denote the submatrix that consists of columns of Φ with indices in T . Let \mathbf{I} denote the identity matrix whose dimension is decided by contexts.

Let \mathbf{x}_S be the best s -terms approximation of \mathbf{x} , where $|S| = s$ and the set S maintains the indices of the s largest magnitude entries in \mathbf{x} .

Consider the general CS model:

$$\mathbf{y} = \Phi \mathbf{x} + \mathbf{e} = \Phi \mathbf{x}_S + \Phi \mathbf{x}_{\bar{S}} + \mathbf{e} = \Phi \mathbf{x}_S + \mathbf{e}', \quad (3)$$

where $\Phi \in \mathbb{R}^{m \times N}$ is a measurement matrix with $m \ll N$, $\mathbf{e} \in \mathbb{R}^m$ is an arbitrary noise, $\mathbf{y} \in \mathbb{R}^m$ is a low-dimensional observation, and $\mathbf{e}' = \Phi \mathbf{x}_{\bar{S}} + \mathbf{e}$ denotes the total perturbation by the sparsity defect $\mathbf{x}_{\bar{S}}$ and measurement error \mathbf{e} .

The definitions of RIP and RIC are given in [2] as follows.

Definition 1: The measurement matrix $\Phi \in \mathbb{R}^{m \times N}$ is said to satisfy the s -order RIP if for any s -sparse signal $\mathbf{x} \in \mathbb{R}^N$

$$(1 - \delta) \|\mathbf{x}\|_2^2 \leq \|\Phi \mathbf{x}\|_2^2 \leq (1 + \delta) \|\mathbf{x}\|_2^2, \quad (4)$$

where $0 \leq \delta \leq 1$. The infimum of δ , denoted by δ_s , is called the s -order RIC of Φ .

$\forall S \subseteq \{1, 2, \dots, N\}, |S| \leq s$, for any eigenvalue $\lambda(\Phi_S^* \Phi_S)$ of $\Phi_S^* \Phi_S$, (4) is equivalent to,

$$1 - \delta_s \leq \lambda(\Phi_S^* \Phi_S) \leq 1 + \delta_s. \quad (5)$$

Then we have,

$$1 - \mu - \mu\delta_s \leq \lambda(\mathbf{I} - \mu\Phi_S^*\Phi_S) \leq 1 - \mu + \mu\delta_s. \quad (6)$$

Then, since $\mathbf{I} - \mu\Phi_S^*\Phi_S$ is hermitian, $\forall \mu \geq 0$, one has

$$\|\mathbf{I} - \mu\Phi_S^*\Phi_S\| = |\lambda(\mathbf{I} - \mu\Phi_S^*\Phi_S)|_{\max} \leq |\mu - 1| + \mu\delta_s. \quad (7)$$

where $\|\mathbf{I} - \mu\Phi_S^*\Phi_S\|$ denotes the spectral norm of $\mathbf{I} - \mu\Phi_S^*\Phi_S$.

Considering the similarity with SP, our theoretical analysis for STP mainly follows the framework the authors developed in [21]. Before our derivations, we should introduce some lemmas which are referenced or developed in [21].

The following two lemmas are used in the derivations of RIC related results.

Lemma 1 (Consequences of the RIP):

- 1) (Monotonicity [2]) For any two positive integers $s \leq s'$, $\delta_s \leq \delta_{s'}$.
- 2) For two vectors $\mathbf{u}, \mathbf{v} \in \mathbb{R}^N$, if $|\text{supp}(\mathbf{u}) \cup \text{supp}(\mathbf{v})| \leq t$, then

$$|\langle \mathbf{u}, (\mathbf{I} - \mu\Phi^*\Phi)\mathbf{v} \rangle| \leq (|\mu - 1| + \mu\delta_t)\|\mathbf{u}\|_2\|\mathbf{v}\|_2; \quad (8)$$

moreover, if $U \subseteq \{1, \dots, N\}$ and $|U \cup \text{supp}(\mathbf{v})| \leq t$, then

$$\|((\mathbf{I} - \mu\Phi^*\Phi)\mathbf{v})_U\|_2 \leq (|\mu - 1| + \mu\delta_t)\|\mathbf{v}\|_2. \quad (9)$$

We omit the proofs of (8) and (9) here for their similarity to the proofs of [21, Lemma 1].

Lemma 2 (Noise perturbation in partial supports [17]): For the general CS model $\mathbf{y} = \Phi\mathbf{x}_S + \mathbf{e}'$ in (3), letting $U \subseteq \{1, \dots, N\}$ and $|U| \leq u$, we have

$$\|(\Phi^*\mathbf{e}')_U\|_2 \leq \sqrt{1 + \delta_u}\|\mathbf{e}'\|_2. \quad (10)$$

The next lemma introduces a simple inequality introduced in [21] which is useful in our derivations.

Lemma 3 ([21]): For nonnegative numbers a, b, c, d, x, y ,

$$(ax + by)^2 + (cx + dy)^2 \leq (\sqrt{a^2 + c^2}x + (b + d)y)^2. \quad (11)$$

Consider the general CS model $\mathbf{y} = \Phi\mathbf{x}_S + \mathbf{e}'$ in (3). Let $T \subseteq \{1, 2, \dots, N\}$ and $|T| = t$. Let \mathbf{z}_p be the solution of the least squares problem $\arg \min_{\mathbf{z} \in \mathbb{R}^N} \{\|\mathbf{y} - \Phi\mathbf{z}\|_2, \text{supp}(\mathbf{z}) \subseteq T\}$. The least squares problem has the following orthogonal properties introduced in [21].

Lemma 4 (Consequences for orthogonality by the RIP [21]): If $\delta_{s+t} < 1$,

$$\|(\mathbf{x}_S - \mathbf{z}_p)_T\|_2 \leq \delta_{s+t} \|\mathbf{x}_S - \mathbf{z}_p\|_2 + \sqrt{1 + \delta_t} \|\mathbf{e}'\|_2 \quad (12)$$

and

$$\|\mathbf{x}_S - \mathbf{z}_p\|_2 \leq \sqrt{\frac{1}{1 - \delta_{s+t}^2}} \|(\mathbf{x}_S)_{\bar{T}}\|_2 + \frac{\sqrt{1 + \delta_t}}{1 - \delta_{s+t}} \|\mathbf{e}'\|_2. \quad (13)$$

Moreover, if $t > s$, define $T_\nabla := \{\text{The indices of the } t - s \text{ smallest magnitude entries of } \mathbf{z}_p \text{ in } T\}$, we have

$$\|(\mathbf{x}_S)_{T_\nabla}\|_2 \leq \sqrt{2} \|(\mathbf{x}_S - \mathbf{z}_p)_T\|_2 \leq \sqrt{2} \delta_{s+t} \|\mathbf{x}_S - \mathbf{z}_p\|_2 + \sqrt{2(1 + \delta_t)} \|\mathbf{e}'\|_2. \quad (14)$$

Throughout the paper, we use the notation (i) stacked over an inequality sign to indicate that the inequality follows from the expression (i) in the paper.

III. ALGORITHM DESCRIPTION AND THEORETICAL ANALYSES

In this section, we give the algorithm description of STP in subsection III-A. Then we give the theoretical guarantee and its proof in subsection III-B. Finally, we show the upper bound of the number of iterations of STP.

A. Algorithm Description

Before the algorithm description of our proposed algorithm STP, we should introduce two algorithms SP and HTP. The main steps of the two algorithms are summarized below.

Algorithm 1 Subspace Pursuit

Input: \mathbf{y}, Φ, s .

Initialization: $S^0 = \emptyset, \mathbf{x}^0 = \mathbf{0}$.

Iteration: At the n -th iteration, go through the following steps.

- 1) $\Delta S = \{s \text{ indices corresponding to the } s \text{ largest magnitude entries in the vector } \Phi^*(\mathbf{y} - \Phi \mathbf{x}^{n-1})\}$.
- 2) $\tilde{S}^n = S^{n-1} \cup \Delta S$.
- 3) $\tilde{\mathbf{x}}^n = \arg \min_{\mathbf{z} \in \mathbb{R}^N} \{\|\mathbf{y} - \Phi \mathbf{z}\|_2, \text{supp}(\mathbf{z}) \subseteq \tilde{S}^n\}$.
- 4) $S^n = \{s \text{ indices corresponding to the } s \text{ largest magnitude elements of } \tilde{\mathbf{x}}^n\}$.
- 5) $\mathbf{x}^n = \arg \min_{\mathbf{z} \in \mathbb{R}^N} \{\|\mathbf{y} - \Phi \mathbf{z}\|_2, \text{supp}(\mathbf{z}) \subseteq S^n\}$.

until the stopping criteria is met.

Output: $\mathbf{x}^n, \text{supp}(\mathbf{x}^n)$.

Algorithm 2 Hard Thresholding Pursuit

Input: \mathbf{y}, Φ, s .

Initialization: $S^0 = \emptyset, \mathbf{x}^0 = \mathbf{0}$.

Iteration: At the n -th iteration, go through the following steps.

- 1) $S^n = \{s \text{ indices corresponding to the } s \text{ largest magnitude entries of } \mathbf{x}^{n-1} + \Phi^*(\mathbf{y} - \Phi \mathbf{x}^{n-1})\}$.
- 2) $\mathbf{x}^n = \arg \min_{\mathbf{z} \in \mathbb{R}^N} \{\|\mathbf{y} - \Phi \mathbf{z}\|_2, \text{supp}(\mathbf{z}) \subseteq S^n\}$.

until the stopping criteria is met.

Output: $\mathbf{x}^n, \text{supp}(\mathbf{x}^n)$.

The main steps of STP are summarized below.

Algorithm 3 Subspace Thresholding Pursuit

Input: $\mathbf{y}, \Phi, s, \alpha, \mu$.

Initialization: $S^0 = \emptyset, \mathbf{x}^0 = \mathbf{0}$.

Iteration: At the n -th iteration, go through the following steps.

- 1) $\Delta S = \{\alpha s \text{ indices corresponding to the } \alpha s \text{ largest magnitude entries in the vector } \Phi^* (\mathbf{y} - \Phi \mathbf{x}^{n-1})\}$.
- 2) $\tilde{S}^n = S^{n-1} \cup \Delta S$.
- 3) $\tilde{\mathbf{x}}^n = \arg \min_{\mathbf{z} \in \mathbb{R}^N} \{\|\mathbf{y} - \Phi \mathbf{z}\|_2, \text{supp}(\mathbf{z}) \subseteq \tilde{S}^n\}$.
- 4) $U^n = \{s \text{ indices corresponding to the } s \text{ largest magnitude elements of } \tilde{\mathbf{x}}^n\}$.
- 5) $\mathbf{u}^n = \{\text{the vector from } \tilde{\mathbf{x}}^n \text{ that keeps the entries of } \tilde{\mathbf{x}}^n \text{ in } U^n \text{ and set all other ones to zero.}\}$
- 6) $S^n = \{s \text{ indices corresponding to the } s \text{ largest magnitude entries of } \mathbf{u}^n + \mu \Phi^* (\mathbf{y} - \Phi \mathbf{u}^n)\}$.
- 7) $\mathbf{x}^n = \arg \min_{\mathbf{z} \in \mathbb{R}^N} \{\|\mathbf{y} - \Phi \mathbf{z}\|_2, \text{supp}(\mathbf{z}) \subseteq S^n\}$.

until the stopping criteria is met.

Output: $\mathbf{x}^n, \text{supp}(\mathbf{x}^n)$.

The STP algorithm is initialized with a trivial signal approximation $\mathbf{x}^0 = \mathbf{0}$ and a trivial support estimate $S^0 = \emptyset$. The parameters α, μ can be adjusted before the algorithm execution. In each iteration, we call steps 1 and 2 ‘‘OMP-like identification’’ since they are common identification steps for all OMP-like algorithms. Such identification steps select the set ΔS of the indices corresponding to the one or several largest entries in the one-dimensional approximation $\Phi^* (\mathbf{y} - \Phi \mathbf{x}^{n-1})$ of the residue $\mathbf{y} - \Phi \mathbf{x}^{n-1}$ and then merge ΔS and the support estimate S^{n-1} of last iteration. Then in step 3, we solve a least squares problem to approximate the original signal \mathbf{x} on the merged set \tilde{S}^n . In steps 4 and 5, we employ a pruning stage by retaining only the s largest entries in the least squares signal approximation $\tilde{\mathbf{x}}$ to produce a new approximation \mathbf{u}^n . The step 6 is a common step for all IHT-like algorithms which is called ‘‘IHT-like identification’’. In the IHT-like identification step, we select the set S^n of indices corresponding to the s largest entries in the vector $\mathbf{u}^n + \mu \Phi^* (\mathbf{y} - \Phi \mathbf{u}^n)$. Finally, we solve a least squares problem again to get the final approximation \mathbf{x}^n in the n -th iteration.

The stopping criteria of iterative greedy algorithms can be selected differently in implementation. We can use the stopping criteria according to the algorithm property, such as ‘‘ $n > s$ ’’ of OMP, ‘‘ $\|\mathbf{y} - \Phi \mathbf{x}^n\|_2 \geq \|\mathbf{y} - \Phi \mathbf{x}^{n-1}\|_2$ ’’ of SP in [10] or ‘‘ $S^{n-1} = S^n$ ’’ of HTP in [17], or use the stopping criteria that is independent from the algorithm itself, which may be ‘‘ $n > n_{\max}$ or $\|\mathbf{y} - \Phi \mathbf{x}^n\|_2 < \varepsilon \|\mathbf{y}\|_2$ ’’. If we know that the algorithm is stable, i.e., as the iteration process continues, the series $\{\|\mathbf{x}^n - \mathbf{x}\|_2, n = 1, 2, 3, \dots\}$ will not diverge, such a criteria provides a tradeoff between accuracy and computational complexity.

OMP-like algorithms and IHT-like algorithms have big difference in the identification steps, but the

representatives SP and HTP of both kinds respectively have nearly the same empirical performance. The main characteristic of the proposed STP algorithm is that we combine the “OMP-like identification” and “IHT-like identification” in one iteration, so as to take full advantage of the virtue of both SP and HTP. In Alg. 3, if we set $\alpha = 1, \mu = 0$, STP degrades to SP; if we set $\alpha = 0, \mu = 1$, STP degrades to HTP (in this case $\mathbf{u}^n = \mathbf{x}^{n-1}$ and the steps 1 to 5 of STP are useless). That is to say, with special parameters α, μ , SP and HTP are two special cases of STP. In order to represent general case and analyze theoretical guarantee conveniently, we set $\alpha = 1$ in the following discussion. The interested readers are encouraged to test other settings of α .

In view of IHT-like algorithms, $\text{supp}(\mathbf{x})$ can lie both in the supports of the median approximation \mathbf{u}^n and the median residue $\mathbf{x} - \mathbf{u}^n$, but the pruning process is only taken in the median estimate \tilde{S}^n . Therefore, after pruning stage, taking a IHT-like identification step may be a good way to give the supports of \mathbf{x} in $S \setminus U^n$ the opportunity to enter into the final support estimate S^n , so as to get a better approximation effect. The weight parameter μ is selected according to user experiences. If μ is large, STP is prone to select the indices of $\text{supp}(\mathbf{x} - \mathbf{u}^n)$; conversely, the indices of $\text{supp}(\mathbf{u}^n)$ is preferred to be selected.

Before our analysis, we emphasize again that unless stated, we set $\alpha = 1$ in this paper.

In Alg. 3, the first two steps and the last step are identical with the corresponding steps of SP in Alg. 1, so the property of the identification step for SP is also suitable for STP. Similar to [21, Lemma 6], we have a lemma for STP as follows.

Lemma 5: In the steps 1 and 2 of STP, we have

$$\|(\mathbf{x}_S)_{\tilde{S}^n}\|_2 \leq \sqrt{2}\delta_{3s}\|\mathbf{x}_S - \mathbf{x}^{n-1}\|_2 + \sqrt{2(1 + \delta_{2s})}\|\mathbf{e}'\|_2.$$

In Alg. 3, the step 6, i.e., the IHT-like identification step also has similar property with steps 1 and 2, which has been developed in Foucart [17] when $\mu = 1$. In our discussion, we generalize the result in [17] to the more general case with $\mu \geq 0$.

Lemma 6 (IHT-like Identification): In the step 6 of STP, we have

$$\|(\mathbf{x}_S)_{\tilde{S}^n}\|_2 \leq \sqrt{2}(|\mu - 1| + \mu\delta_{3s})\|\mathbf{x}_S - \mathbf{u}^n\|_2 + \sqrt{2(1 + \delta_{2s})}\mu\|\mathbf{e}'\|_2.$$

Proof: In the step 6 of the n -th iteration, S^n is the set of the s indices corresponding to the s largest magnitude entries in $\mathbf{u}^n + \mu\Phi^*(\mathbf{y} - \Phi\mathbf{u}^n)$. Thus,

$$\|(\mathbf{u}^n + \mu\Phi^*(\mathbf{y} - \Phi\mathbf{u}^n))_S\|_2 \leq \|(\mathbf{u}^n + \mu\Phi^*(\mathbf{y} - \Phi\mathbf{u}^n))_{S^n}\|_2. \quad (15)$$

Removing the common coordinates in $S \cap S^n$ and noticing that $\mathbf{y} = \Phi \mathbf{x}_S + \mathbf{e}'$, we have

$$\|(\mathbf{u}^n + \mu \Phi^*(\mathbf{y} - \Phi \mathbf{u}^n))_{S \setminus S^n}\|_2 \leq \|(\mathbf{u}^n + \mu \Phi^*(\mathbf{y} - \Phi \mathbf{u}^n))_{S^n \setminus S}\|_2. \quad (16)$$

For the right-hand side of (16), noticing that $(\mathbf{x}_S)_{S^n \setminus S} = \mathbf{0}$, we have

$$\begin{aligned} \|(\mathbf{u}^n + \mu \Phi^*(\mathbf{y} - \Phi \mathbf{u}^n))_{S^n \setminus S}\|_2 &= \|(\mathbf{u}^n + \mu \Phi^* \Phi (\mathbf{x}_S - \mathbf{u}^n) + \mu \Phi^* \mathbf{e}')_{S^n \setminus S}\|_2 \\ &\leq \|((\mu \Phi^* \Phi - \mathbf{I})(\mathbf{x}_S - \mathbf{u}^n))_{S^n \setminus S}\|_2 + \|(\mu \Phi^* \mathbf{e}')_{S^n \setminus S}\|_2. \end{aligned} \quad (17)$$

For the left-hand side of (16), noticing that $(\mathbf{x}_S)_{S \setminus S^n} = (\mathbf{x}_S)_{\overline{S^n}}$, we have

$$\begin{aligned} \|(\mathbf{u}^n + \mu \Phi^*(\mathbf{y} - \Phi \mathbf{u}^n))_{S \setminus S^n}\|_2 &= \|(\mathbf{u}^n + \mu \Phi^* \Phi (\mathbf{x}_S - \mathbf{u}^n) + \mu \Phi^* \mathbf{e}' - \mathbf{x}_S + \mathbf{x}_S)_{S \setminus S^n}\|_2 \\ &\geq \|(\mathbf{x}_S)_{\overline{S^n}}\|_2 - \|((\mu \Phi^* \Phi - \mathbf{I})(\mathbf{x}_S - \mathbf{u}^n))_{S \setminus S^n}\|_2 - \|(\mu \Phi^* \mathbf{e}')_{S \setminus S^n}\|_2. \end{aligned} \quad (18)$$

Combining (16), (17) and (18), we have

$$\begin{aligned} \|(\mathbf{x}_S)_{\overline{S^n}}\|_2 &\leq \|((\mu \Phi^* \Phi - \mathbf{I})(\mathbf{x}_S - \mathbf{u}^n))_{S^n \setminus S}\|_2 + \|(\mu \Phi^* \mathbf{e}')_{S^n \setminus S}\|_2 \\ &\quad + \|((\mu \Phi^* \Phi - \mathbf{I})(\mathbf{x}_S - \mathbf{u}^n))_{S \setminus S^n}\|_2 + \|(\mu \Phi^* \mathbf{e}')_{S \setminus S^n}\|_2 \\ &\leq \sqrt{2} \|((\mu \Phi^* \Phi - \mathbf{I})(\mathbf{x}_S - \mathbf{u}^n))_{(S^n \setminus S) \cup (S \setminus S^n)}\|_2 + \sqrt{2} \|(\mu \Phi^* \mathbf{e}')_{(S^n \setminus S) \cup (S \setminus S^n)}\|_2 \end{aligned} \quad (19)$$

$$\leq \sqrt{2}(|\mu - 1| + \mu \delta_{3s}) \|\mathbf{x}_S - \mathbf{u}^n\|_2 + \sqrt{2(1 + \delta_{2s})} \mu \|\mathbf{e}'\|_2. \quad (20)$$

where the inequality (19) is from the Cauchy-Schwartz inequality. ■

B. The Theoretical Guarantee

In this subsection, we establish the sufficient condition to guarantee STP to converge in realistic situation, i.e., considering the general CS model $\mathbf{y} = \Phi \mathbf{x}_S + \mathbf{e}'$ in (3) directly. The conclusion in realistic situation specialize to the idealized situation simply by setting $\mathbf{e}' = \mathbf{0}$. In fact, setting $\mathbf{e}' = \mathbf{0}$ inside our derivations would simplify them considerably.

Theorem 1: For the general CS model $\mathbf{y} = \Phi \mathbf{x}_S + \mathbf{e}'$ in (3), if $\frac{1}{1 - \delta_{3s}} - \frac{1 + \delta_{3s}}{2\delta_{3s}\sqrt{1 + 2\delta_{3s}^2}} < \mu < 1$, or $1 < \mu < \frac{1}{1 + \delta_{3s}} + \frac{1 - \delta_{3s}}{2\delta_{3s}\sqrt{1 + 2\delta_{3s}^2}}$, or $\mu = 1$ with $\delta_{3s} < 0.5340$, then the sequence of \mathbf{x}^n defined by STP satisfies

$$\|\mathbf{x}_S - \mathbf{x}^n\|_2 \leq \rho^n \|\mathbf{x}_S\|_2 + \tau \|\mathbf{e}'\|_2, \quad (21)$$

where

$$\rho = \frac{2\delta_{3s}(|\mu - 1| + \mu \delta_{3s})\sqrt{1 + 2\delta_{3s}^2}}{1 - \delta_{3s}^2} < 1, \quad (22)$$

$$(1 - \rho)\tau = \left(\frac{\sqrt{2 + \sqrt{2}\delta_{3s}}(|\mu - 1| + \mu\delta_{3s})}{\sqrt{1 - \delta_{3s}^2}} + 1 \right) \frac{\sqrt{2(1 - \delta_{3s})} + \sqrt{1 + \delta_{3s}}}{1 - \delta_{3s}} + \frac{\sqrt{4 + \sqrt{2}}(|\mu - 1| + \mu\delta_{3s})}{\sqrt{1 - \delta_{3s}}}. \quad (23)$$

Proof:

The steps 1 and 2 are the OMP-like identification steps. By Lemma 5, in the n -th iteration, we have

$$\|(\mathbf{x}_S)_{\bar{S}^n}\|_2 \leq \sqrt{2}\delta_{3s}\|\mathbf{x}_S - \mathbf{x}^{n-1}\|_2 + \sqrt{2(1 + \delta_{2s})}\|\mathbf{e}'\|_2. \quad (24)$$

The step 3 of the n -th iteration is a procedure of solving a least squares problem. Letting $T = \tilde{S}^n$ and $\mathbf{z}_p = \tilde{\mathbf{x}}^n$, $t = 2s$, by (13) of Lemma 4, we have

$$\|\mathbf{x}_S - \tilde{\mathbf{x}}^n\|_2 \leq \sqrt{\frac{1}{1 - \delta_{3s}^2}}\|(\mathbf{x}_S)_{\tilde{S}^n}\|_2 + \frac{\sqrt{1 + \delta_{2s}}}{1 - \delta_{3s}}\|\mathbf{e}'\|_2. \quad (25)$$

Then combining (24) and (25) and magnifying δ_{2s} to δ_{3s} by Lemma 1, we have

$$\|\mathbf{x}_S - \tilde{\mathbf{x}}^n\|_2 \leq \sqrt{\frac{2\delta_{3s}^2}{1 - \delta_{3s}^2}}\|\mathbf{x}_S - \mathbf{x}^{n-1}\|_2 + \frac{\sqrt{2(1 - \delta_{3s})} + \sqrt{1 + \delta_{3s}}}{1 - \delta_{3s}}\|\mathbf{e}'\|_2. \quad (26)$$

In the step 4 of the n -th iteration, define $S_\nabla := \tilde{S}^n \setminus U^n$, where S_∇ contains the indices of the s smallest entries in $\tilde{\mathbf{x}}^n$. Letting $T = \tilde{S}^n$ and $\mathbf{z}_p = \tilde{\mathbf{x}}^n$, $t = 2s$, $T_\nabla = S_\nabla$, by (14) of Lemma 4, we have that

$$\|(\mathbf{x}_S)_{S_\nabla}\|_2 \leq \sqrt{2}\delta_{3s}\|\mathbf{x}_S - \tilde{\mathbf{x}}^n\|_2 + \sqrt{2(1 + \delta_{2s})}\|\mathbf{e}'\|_2. \quad (27)$$

Let $\tau_1 = \frac{\sqrt{2(1 - \delta_{3s})} + \sqrt{1 + \delta_{3s}}}{1 - \delta_{3s}}$ and $\tau_2 = \sqrt{1 + \delta_{3s}}$. Dividing \bar{U}^n into two disjoint parts: S_∇ and \bar{S}^n , we have

$$\begin{aligned} \|(\mathbf{x}_S)_{\bar{U}^n}\|_2^2 &= \|(\mathbf{x}_S)_{S_\nabla}\|_2^2 + \|(\mathbf{x}_S)_{\bar{S}^n}\|_2^2 \\ &\stackrel{(27),(24)}{\leq} 2(\delta_{3s}\|\mathbf{x}_S - \tilde{\mathbf{x}}^n\|_2 + \tau_2\|\mathbf{e}'\|_2)^2 + 2(\delta_{3s}\|\mathbf{x}_S - \mathbf{x}^{n-1}\|_2 + \tau_2\|\mathbf{e}'\|_2)^2 \\ &\stackrel{(26)}{\leq} 2\left(\delta_{3s}\sqrt{\frac{2\delta_{3s}^2}{1 - \delta_{3s}^2}}\|\mathbf{x}_S - \mathbf{x}^{n-1}\|_2 + (\delta_{3s}\tau_1 + \tau_2)\|\mathbf{e}'\|_2\right)^2 + 2(\delta_{3s}\|\mathbf{x}_S - \mathbf{x}^{n-1}\|_2 + \tau_2\|\mathbf{e}'\|_2)^2 \\ &\stackrel{(11)}{\leq} 2\left(\sqrt{\frac{2\delta_{3s}^4}{1 - \delta_{3s}^2}} + \delta_{3s}^2\|\mathbf{x}_S - \mathbf{x}^{n-1}\|_2 + ((\delta_{3s}\tau_1 + \tau_2) + \tau_2)\|\mathbf{e}'\|_2\right)^2 \\ &= 2\left(\sqrt{\frac{\delta_{3s}^2(1 + \delta_{3s}^2)}{1 - \delta_{3s}^2}}\|\mathbf{x}_S - \mathbf{x}^{n-1}\|_2 + (\delta_{3s}\tau_1 + 2\tau_2)\|\mathbf{e}'\|_2\right)^2, \end{aligned}$$

which implies that

$$\|(\mathbf{x}_S)_{\bar{U}^n}\|_2 \leq \sqrt{\frac{2\delta_{3s}^2(1 + \delta_{3s}^2)}{1 - \delta_{3s}^2}}\|\mathbf{x}_S - \mathbf{x}^{n-1}\|_2 + \sqrt{2}(\delta_{3s}\tau_1 + 2\tau_2)\|\mathbf{e}'\|_2. \quad (28)$$

In the step 5 of the n -th iteration, since \mathbf{u}^n is obtained by keeping the s largest magnitude entries of $\tilde{\mathbf{x}}^n$, we have

$$\begin{aligned}
& \|(\mathbf{x}_S - \mathbf{u}^n)_{U^n}\|_2 \leq \|(\mathbf{x}_S - \tilde{\mathbf{x}}^n)_{\tilde{S}^n}\|_2 \\
& \stackrel{(12)}{\leq} \delta_{3s} \|\mathbf{x}_S - \tilde{\mathbf{x}}^n\|_2 + \sqrt{1 + \delta_{3s}} \|\mathbf{e}'\|_2 \\
& \stackrel{(26)}{\leq} \sqrt{\frac{2\delta_{3s}^4}{1 - \delta_{3s}^2}} \|\mathbf{x}_S - \mathbf{x}^{n-1}\|_2 + \left(\delta_{3s} \frac{\sqrt{2(1 - \delta_{3s})} + \sqrt{1 + \delta_{3s}}}{1 - \delta_{3s}} + \sqrt{1 + \delta_{3s}} \right) \|\mathbf{e}'\|_2 \\
& = \sqrt{\frac{2\delta_{3s}^4}{1 - \delta_{3s}^2}} \|\mathbf{x}_S - \mathbf{x}^{n-1}\|_2 + (\delta_{3s}\tau_1 + \tau_2) \|\mathbf{e}'\|_2.
\end{aligned} \tag{29}$$

Dividing $\text{supp}(\mathbf{x}_S - \mathbf{u}^n)$ into two disjoint parts: $U^n, \overline{U^n}$, and noticing that $(\mathbf{x}_S - \mathbf{u}^n)_{\overline{U^n}} = (\mathbf{x}_S)_{\overline{U^n}}$, we have

$$\begin{aligned}
& \|\mathbf{x}_S - \mathbf{u}^n\|_2^2 = \|(\mathbf{x}_S - \mathbf{u}^n)_{U^n}\|_2^2 + \|(\mathbf{x}_S - \mathbf{u}^n)_{\overline{U^n}}\|_2^2 = \|(\mathbf{x}_S - \mathbf{u}^n)_{U^n}\|_2^2 + \|(\mathbf{x}_S)_{\overline{U^n}}\|_2^2 \\
& \stackrel{(29),(28)}{\leq} \left(\sqrt{\frac{2\delta_{3s}^4}{1 - \delta_{3s}^2}} \|\mathbf{x}_S - \mathbf{x}^{n-1}\|_2 + (\delta_{3s}\tau_1 + \tau_2) \|\mathbf{e}'\|_2 \right)^2 \\
& \quad + \left(\sqrt{\frac{2\delta_{3s}^2(1 + \delta_{3s}^2)}{1 - \delta_{3s}^2}} \|\mathbf{x}_S - \mathbf{x}^{n-1}\|_2 + \sqrt{2}(\delta_{3s}\tau_1 + 2\tau_2) \|\mathbf{e}'\|_2 \right)^2 \\
& \stackrel{(11)}{\leq} \left(\sqrt{\frac{2\delta_{3s}^2(1 + 2\delta_{3s}^2)}{1 - \delta_{3s}^2}} \|\mathbf{x}_S - \mathbf{x}^{n-1}\|_2 + ((\sqrt{2} + 1)\delta_{3s}\tau_1 + (2\sqrt{2} + 1)\tau_2) \|\mathbf{e}'\|_2 \right)^2,
\end{aligned}$$

or

$$\|\mathbf{x}_S - \mathbf{u}^n\|_2 \leq \sqrt{\frac{2\delta_{3s}^2(1 + 2\delta_{3s}^2)}{1 - \delta_{3s}^2}} \|\mathbf{x}_S - \mathbf{x}^{n-1}\|_2 + ((\sqrt{2} + 1)\delta_{3s}\tau_1 + (2\sqrt{2} + 1)\tau_2) \|\mathbf{e}'\|_2. \tag{30}$$

The step 6 of STP is the IHT-like identification step. By Lemma 6, in the n -th iteration, we have

$$\|(\mathbf{x}_S)_{\overline{S}^n}\|_2 \leq \sqrt{2}(|\mu - 1| + \mu\delta_{3s}) \|\mathbf{x}_S - \mathbf{u}^n\|_2 + \sqrt{2(1 + \delta_{2s})}\mu \|\mathbf{e}'\|_2. \tag{31}$$

The step 7 of the n -th iteration is a procedure of solving a least squares problem. Letting $T = S^n$ and $\mathbf{z}_p = \mathbf{x}^n$, $t = s$, by (13) of Lemma 4, we have

$$\|\mathbf{x}_S - \mathbf{x}^n\|_2 \leq \sqrt{\frac{1}{1 - \delta_{2s}^2}} \|(\mathbf{x}_S)_{\overline{S}^n}\|_2 + \frac{\sqrt{1 + \delta_s}}{1 - \delta_{2s}} \|\mathbf{e}'\|_2. \tag{32}$$

Combing (30),(31) and (32), and magnifying δ_s, δ_{2s} to δ_{3s} by Lemma 1, we have

$$\|\mathbf{x}_S - \mathbf{x}^n\|_2 \leq \rho \|\mathbf{x}_S - \mathbf{x}^{n-1}\|_2 + (1 - \rho)\tau \|\mathbf{e}'\|_2. \tag{33}$$

where ρ and τ is respectively referred to (22) and (23). Hence, (21) follows by recursively using the above inequality when $\rho < 1$.

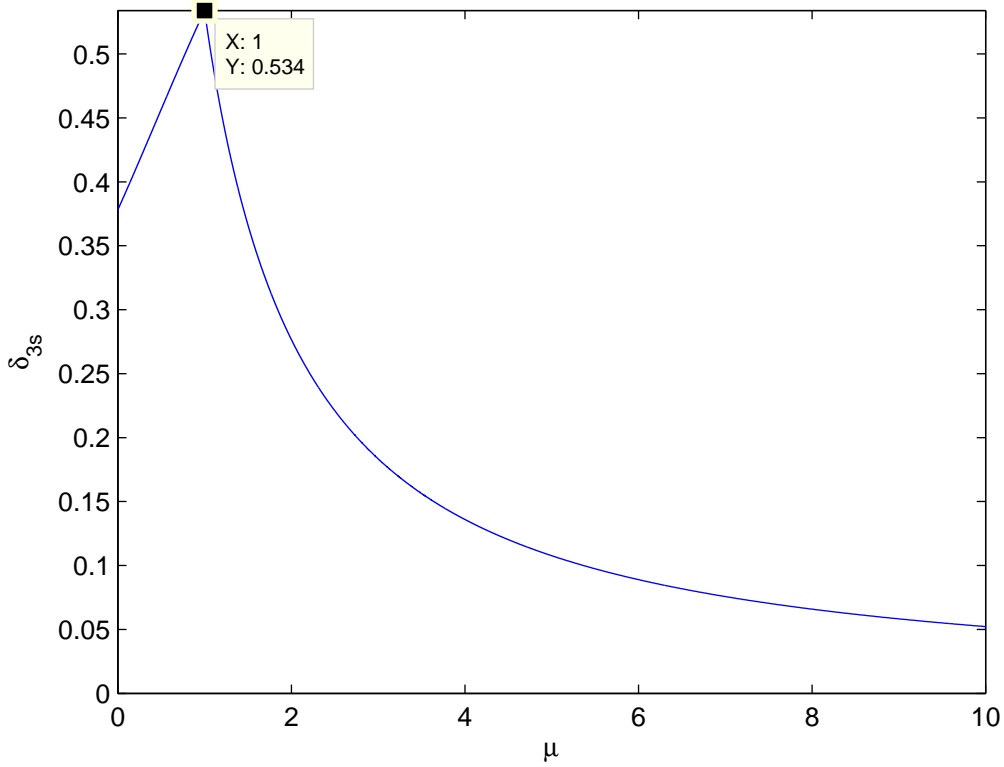


Figure 1. The upper bound of δ_{3s} as μ changes

When $\mu < 1$, $\rho < 1$ is equivalent to $\frac{1}{1 - \delta_{3s}} - \frac{1 + \delta_{3s}}{2\delta_{3s}\sqrt{1 + 2\delta_{3s}}} < \mu < 1$; when $\mu > 1$, $\rho < 1$ is equivalent to $1 < \mu < \frac{1}{1 + \delta_{3s}} + \frac{1 - \delta_{3s}}{2\delta_{3s}\sqrt{1 + 2\delta_{3s}^2}}$; when $\mu = 1$, $\rho < 1$ is equivalent to $\delta_{3s} < 0.5340$. Thus we finish the proof. ■

In Fig. 1, we plot the upper bound of δ_{3s} as μ changes. From Fig. 1, we know that when $\mu = 1$, we get the best theoretical guarantee $\delta_{3s} < 0.5340$ of STP. So far, the best theoretical guarantee for the kind of iterative greedy algorithms is $\delta_{3s} < \frac{1}{\sqrt{3}} \approx 0.5773$ of HTP and IHT, so STP with $\mu = 1$ attains one of the best theoretical guarantees in iterative greedy algorithms. In addition, when $\mu \neq 1$, we can still get a theoretical guarantee comparable to that of ℓ_1 minimization, i.e., the RIC is bound by a positive constant. As we will see in Section IV, the optimal μ which make STP attain optimal empirical performance is the one that is larger than 1 in most cases.

C. The number of iterations

Now we consider the number of iterations of STP to reconstruct s -sparse signals in noiseless environment. It shows that the convergence requires a finite number of iterations.

Theorem 2: Assume that the measurement matrix Φ and the parameter μ satisfy $\rho = \frac{2\delta_{3s}(|\mu-1|+\mu\delta_{3s})\sqrt{1+2\delta_{3s}^2}}{1-\delta_{3s}^2} < 1$, particularly when $\mu = 1$, $\delta_{3s} < 0.5340$, then any s -sparse vector $\mathbf{x} \in \mathbb{R}^N$ is reconstructed by STP with $\mathbf{y} = \Phi\mathbf{x}$ in at most

$$\min \left\{ \left\lceil \frac{\ln \|\mathbf{x}\|_2 / \xi}{\ln 1/\rho} \right\rceil, \left\lceil \frac{1.5s}{\ln 1/\rho} \right\rceil \right\} \text{ iterations.} \quad (34)$$

where ξ is defined as the smallest magnitude of all the entries in \mathbf{x} .

Proof: On the one hand, considering the similarity with HTP, our proof for the number of iterations of STP mainly follows the proof of [17, corollary 3.6]. According to the steps 6 and 7 of STP, if $S^n = S$, then we will get the exact solution by solving the least squares problem in step 7. For all $i \in S$ and $j \in \bar{S}$, a sufficient condition to guarantee $S^n = S$ in step 6 is

$$|(\mathbf{u}^n + \mu\Phi^*(\mathbf{y} - \Phi\mathbf{u}^n))_i| > |(\mathbf{u}^n + \mu\Phi^*(\mathbf{y} - \Phi\mathbf{u}^n))_j| = |((\mu\Phi^*\Phi - \mathbf{I})(\mathbf{x} - \mathbf{u}^n))_j|. \quad (35)$$

We observe that

$$|(\mathbf{u}^n + \mu\Phi^*(\mathbf{y} - \Phi\mathbf{u}^n))_i| = |(\mathbf{u}^n + \mu\Phi^*(\mathbf{y} - \Phi\mathbf{u}^n) - \mathbf{x} + \mathbf{x})_i| \geq \xi - |((\mu\Phi^*\Phi - \mathbf{I})(\mathbf{x} - \mathbf{u}^n))_i|. \quad (36)$$

Then, we show that

$$\begin{aligned} & |((\mu\Phi^*\Phi - \mathbf{I})(\mathbf{x} - \mathbf{u}^n))_i| + |((\mu\Phi^*\Phi - \mathbf{I})(\mathbf{x} - \mathbf{u}^n))_j| \\ & \leq \sqrt{2}((\mu\Phi^*\Phi - \mathbf{I})(\mathbf{x} - \mathbf{u}^n))_{i \cup j} \\ & \leq \sqrt{2}(|\mu - 1| + \mu\delta_{2s+2})\|\mathbf{x} - \mathbf{u}^n\|_2 \\ & \leq \sqrt{2}(|\mu - 1| + \mu\delta_{3s})\|\mathbf{x} - \mathbf{u}^n\|_2 \\ & \leq \sqrt{2}(|\mu - 1| + \mu\delta_{3s})\sqrt{\frac{2\delta_{3s}^2(1+2\delta_{3s}^2)}{1-\delta_{3s}^2}}\|\mathbf{x} - \mathbf{x}^{n-1}\|_2 \\ & \leq \sqrt{2}(|\mu - 1| + \mu\delta_{3s})\sqrt{\frac{2\delta_{3s}^2(1+2\delta_{3s}^2)}{1-\delta_{3s}^2}}\rho^{n-1}\|\mathbf{x}\|_2 \\ & = \sqrt{(1-\delta_{3s}^2)}\rho^n\|\mathbf{x}\|_2 \\ & \leq \rho^n\|\mathbf{x}\|_2. \end{aligned} \quad (37)$$

So (35) is satisfied as soon as

$$\xi \geq \rho^n\|\mathbf{x}\|_2. \quad (38)$$

Then the smallest n is

$$\left\lceil \frac{\ln \|\mathbf{x}\|_2 / \xi}{\ln 1/\rho} \right\rceil. \quad (39)$$

On the other hand, assuming that x is s -sparse and setting $\mathbf{e}' = \mathbf{0}$, combining (30) and (31), we have

$$\|\mathbf{x}_{\overline{S}^n}\|_2 \leq 2(|\mu - 1| + \mu\delta_{3s})\delta_{3s}\sqrt{\frac{1 + 2\delta_{3s}^2}{1 - \delta_{3s}^2}}\|\mathbf{x} - \mathbf{x}^{n-1}\|_2. \quad (40)$$

Setting $\mathbf{e}' = \mathbf{0}$ and substituting $n - 1$ for n in (32), one has

$$\|\mathbf{x} - \mathbf{x}^{n-1}\|_2 \leq \sqrt{\frac{1}{1 - \delta_{2s}^2}}\|\mathbf{x}_{\overline{S}^{n-1}}\|_2. \quad (41)$$

Combining (40) and (41) and magnifying δ_{2s} to δ_{3s} , we have

$$\|\mathbf{x}_{\overline{S}^n}\|_2 \leq \rho\|\mathbf{x}_{\overline{S}^{n-1}}\|_2. \quad (42)$$

where ρ referred to (22).

(42) has the same form with [10, Theorem 2 (6)], but different geometry rate ρ , so [10, Theorem 8] is also suitable for STP by using the new ρ in (22) instead of the corresponding one “ c_K ” in [10]. So any s -sparse vector $\mathbf{x} \in \mathbb{R}^N$ is reconstructed by STP with $\mathbf{y} = \Phi\mathbf{x}$ in at most

$$\left\lceil \frac{1.5s}{\ln 1/\rho} \right\rceil. \quad (43)$$

Combining (39) and (43), then we get Theorem 2. ■

Compared with SP, STP adds steps 5 and 6. The runtime of step 5 is negligible and the computational complexity of step 6 in STP is comparable to step 1, i.e., the OMP-identification step, so the computational complexity analysis for SP in [10] is also suitable for STP. Generally, STP has comparable computational complexity with SP. In each iteration, STP needs an extra computational step, but it has less number of iterations than SP since it has better convergence rate ρ than SP under the same measurement matrix.

IV. SIMULATIONS AND ANALYSES

The characteristic that makes STP different is its empirical performance. The theoretical guarantees in terms of RICs provide us the intuition of the worst-case performance of reconstruction algorithms. But it does not say much about empirical performance since the theoretical guarantee by RIP is very weak (see the “strong phase transition curve” in [24]) and there is no efficient way to verify the RIC condition. In this section, we display the empirical performance of the proposed STP algorithms with different μ by comparing the performance measures between STP and other state-of-the-art algorithms, such as the exact reconstruction rate, the average number of iterations and the average runtime. In our simulations, we use the testing strategy in [10], [25] which measures the effectiveness of reconstruction algorithms by checking

the exact reconstruction rate in the noiseless environment. By comparing the maximal sparsity level of the underlying sparse signals at which the perfect reconstruction is ensured (this point is often called critical sparsity [10]), accuracy of the reconstruction can be compared empirically. In our simulations, we consider OMP, the representatives of OMP-like algorithms SP and CoSaMP, the representatives of IHT-like algorithms NIHT and HTP, the ℓ_1 minimization and STP with different μ ($\mu = 1, 1.5, 2, 2.5, 3, 3.5$). We let OMP execute s steps. For other greedy algorithms, we use a common stopping criteria “ $n > 200$ or $\|\mathbf{y} - \Phi\mathbf{x}^n\|_2 < 10^{-10}\|\mathbf{y}\|_2$ ”. For ℓ_1 minimization, we use the default setting in the ℓ_1 -magic package (<http://users.ece.gatech.edu/~justin/l1magic/>). Generally speaking, in realistic situation, the general case may be $m \ll N$, thus selecting a relatively small undersampling ratio such as $\tau = \frac{m}{N} = 0.1$ may give us a better intuition about empirical performance. Therefore, in each trial, we construct $m \times N$ ($m = 100, N = 1000$) measurement matrix Φ with entries drawn independently from Gaussian distribution $\mathbb{N}(0, \frac{1}{m})$. In addition, we generate an s -sparse vector \mathbf{x} whose supports are chosen at random. Two types of sparse signals are considered: Gaussian signals and CARS signals. Each nonzero element of Gaussian signals is drawn from standard Gaussian distribution and that in CARS signal is from the set $\{1, -1\}$ uniformly at random. For each reconstruction algorithm, we perform 2,000 independent trials and plot the exact reconstruction rate, the average number of iterations (only for NIHT, HTP, SP, CoSaMP, STP) and the average runtime in y -axis as the sparsity s changes in x -axis. In order to compare the runtime of different greedy algorithms fairly, we implement all the greedy algorithms in our simulations in the same way. Perhaps these implementations may not be optimal.

In each figure, we plot three curves of STP with three different μ : $\mu = 1$, $\mu = \mu_*$, $\mu = \mu_* + 0.5$, where μ_* stands for the μ that makes STP have optimal empirical performance. In Fig. 2(a), we show that in Gaussian signal case, the critical sparsity of STP with μ_* (in this case $\mu_* = 3$) exceeds all the other algorithms greatly. In Fig. 2(b), we show that in CARS signal case, the empirical performance of STP with μ_* (in this case $\mu_* = 2.5$) exceeds that of all the other algorithms, even including ℓ_1 minimization. To the best of our knowledge, all the existing iterative greedy algorithms perform worse than ℓ_1 minimization in CARS signal case. While, STP with μ_* breaks the limitation if we sample the original signal with relatively practical undersampling ratio such as $\tau = 0.1$. Meanwhile, it demonstrates the iterative greedy algorithms’ potential to reconstruct Gaussian signals sufficiently.

In Fig. 3(a) and Fig. 3(b), we compare the number of iterations in both Gaussian signal case and

CARS signal case (We exclude OMP and ℓ_1 minimization since standard OMP executes exact k steps and the iteration process of ℓ_1 minimization is different in essence from that of iterative greedy algorithms.). We show that the numbers of iterations of STP with different μ are all less than other iterative greedy algorithms when the sparsity s is a little large ($s \geq 3$ in Gaussian signal case; $s \geq 7$ in CARS signal case.). Therefore, the IHT-like identification step introduced in STP adds extra computational time in each iteration, but it can accelerate the iteration process relative to SP.

In Fig. 4(a) and Fig. 4(b), we display the average runtime of all algorithms. The results of ℓ_1 minimization are not displayed in the two local views since the runtime of ℓ_1 minimization is more than order of magnitude higher than that of all other algorithms. We show that the average runtime of STP is comparative to other algorithms in general. When s is a little large, STP has less average time than SP. In addition, we show that although solving a least squares problem is time-consuming, the average runtime of the algorithms with least squares steps can be reduced greatly relative to the kind of algorithms such as NIHT with no least squares steps since least squares steps decrease the number of iterations considerably.

Furthermore, we notice that STP has its best theoretical guarantee $\delta_{3s} < 0.5340$ when $\mu = 1$, but in view of empirical performance, μ_* is larger than 1. In our simulations, let μ change with step size 0.5, for Gaussian signals, μ_* is 3; for CARS signals, μ_* is 2.5. The similar case also happens in the variant NIHT of IHT. NIHT has better empirical performance than IHT, but its theoretical guarantee is worse than that of IHT. On the one hand, the RIC upper bounds for different algorithms are limited by derivation skills; on the other hand, the RIC condition is only the sufficient condition to guarantee sparse recovery, even if δ_{2s} approximates 1, we still can't say that our algorithm can't reconstruct s -sparse signals uniformly under some specified measurement matrix (see the example in [26]). Therefore, theoretical guarantee tells us how bad a algorithm will not be, but the more important measure in practice may be empirical performance.

Table II

THE CRITICAL SPARSITY OF ALGORITHMS UNDER GAUSSIAN MEASUREMENT MATRICES WITH DIFFERENT SIZES IN GAUSSIAN SIGNAL CASE.

Algorithms	OMP	ℓ_1	SP	CoSaMP	NIHT	HTP	STP1	STP1.5	STP2	STP2.5	STP3	STP3.5
Critical Sparsity(100×3000)	8	9	10	9	10	12	11	14	16	19	19	16
Critical Sparsity(100×1000)	10	12	13	13	12	14	15	18	22	24	24	22
Critical Sparsity(200×1000)	24	36	46	42	38	44	50	56	58	64	68	64
Critical Sparsity(300×1000)	47	68	83	80	68	83	89	98	107	116	122	116
Critical Sparsity(400×1000)	57	107	127	127	107	122	137	152	167	172	172	162
Critical Sparsity(500×1000)	72	157	197	162	152	177	202	217	232	227	222	217
Critical Sparsity(600×1000)	87	222	287	217	217	237	288	287	287	282	277	267

Table III

THE CRITICAL SPARSITY OF ALGORITHMS UNDER GAUSSIAN MEASUREMENT MATRICES WITH DIFFERENT SIZES IN CARS SIGNAL CASE.

Algorithms	OMP	ℓ_1	SP	CoSaMP	NIHT	HTP	STP1	STP1.5	STP2	STP2.5	STP3	STP3.5
Critical Sparsity(100×3000)	4	9	5	6	7	6	7	8	10	11	10	9
Critical Sparsity(100×1000)	5	13	10	9	9	8	11	11	13	14	14	13
Critical Sparsity(200×1000)	12	38	31	31	29	29	31	36	36	37	37	35
Critical Sparsity(300×1000)	18	68	58	58	52	52	60	64	68	68	64	60
Critical Sparsity(400×1000)	23	110	95	95	71	80	98	104	104	104	104	98
Critical Sparsity(500×1000)	30	166	138	130	102	118	142	150	142	142	142	134
Critical Sparsity(600×1000)	42	234	190	182	142	150	194	198	194	190	190	186

Finally, we focus on the the key performance measure: critical sparsity in exact reconstruction rate curve. Table II and III show the critical sparsity of all the algorithms in our simulations under Gaussian measurement matrices with different sizes in Gaussian signal case and CARS signal case respectively. In both tables, STP_c stands for STP with $\mu = c$ and in the first columns of both tables, the formulae $m \times N$ ($m = 100, \dots, 600, N = 1000, 3000$) in brackets denote the sizes of the Gaussian measurement matrices we used. In each row, there are two boldfaced numbers, one stands for the maximal critical sparsity among the existing algorithms, the other the maximal critical sparsity among all the STP algorithms with different μ . When there exist two or more STP algorithms with different μ having identical critical sparsity, we highlight the critical sparsity of the STP algorithm which has better exact reconstruction rate when the signal sparsity is larger than critical sparsity.

Firstly, from Tables II and III, we find that the optimal μ that makes STP perform best is bound in a limited range, so in practice tuning the value of μ is easy. In fact, from the two tables, in Gaussian signal case, when τ is relatively practical, such as $\tau \leq 0.3$, if we choose μ with step size 0.5, the optimal μ is 3; in CARS signal case, in similar setting ($\tau \leq 0.2$ and choose μ with step size 0.5), the optimal μ is 2.5. Secondly, we notice that in all the cases ($\tau = 0.033, 0.1, 0.2, 0.3, 0.4, 0.5, 0.6$), STP with optimal μ outperforms all the other greedy algorithms when reconstructing both Gaussian signals and CARS signals. When compared with ℓ_1 minimization, STP with μ_* performs worse than ℓ_1 minimization obviously only when $\tau \geq 0.4$ and the signal type is CARS. In other cases, STP with μ_* has the best empirical performance. In addition, we notice that μ_* is different when reconstructing Gaussian signals and CARS signals. But since the influence of μ to the empirical performance of STP is asymptotical, we can select a μ between the μ_* in Gaussian signal case and μ_* in CARS signal case in practice.

In conclusion, by our simulations, STP with μ_* has excellent empirical performance. Compared with all other reconstruction algorithms, it is more appropriate to realistic application—the smaller the under-

sampling ratio is, the more obvious the superiority of STP with μ_* is. Compared with ℓ_1 minimization, the computational complexity of STP with μ_* is more than order of magnitude lower than that of ℓ_1 minimization. But it has twice higher empirical performance in Gaussian signal case and a little higher empirical performance in CARS signal case than ℓ_1 minimization when the undersampling ratio is small. Compared with other state-of-the-art algorithms, the empirical performance of STP with μ_* exceeds them greatly both in Gaussian signal case and CARS signal case. Therefore, STP with μ_* has good application prospect.

V. SOME EXTENDED STUDY

In this section, we discuss some extended study. Firstly, from the last row of Table II, the critical sparsity of STP with $\mu_* = 1$ is 288 which approximates the limitation $\lceil m/2 \rceil = 300$ well. But in our simulations, when the sparsity s is a little larger than the critical sparsity 288, the exact reconstruction rate will decrease to zero quickly. The reason we find is “overfitting”. That is to say, when the cardinality of \tilde{S}^n in step 3 of Alg. 3 approximate m enough or exceed m , the least squares problem in step 3 will be an ill-posed problem. Then the solution $\tilde{\mathbf{x}}^n$ may not be unique, thus the principle of STP is broken. In subsection V-A, we propose a simple but effective way to solve the overfitting problem. Secondly, from the above sections, we know that STP is only a simple combination of SP and IHT. A direct idea may be to combine other similar iterative greedy algorithms and IHT. In subsection V-B, we show the improvement by the IHT-like identification step to four other iterative greedy algorithms: CoSaMP, HTP, SAMP and FBP.

A. A method to eliminate overfitting

In order to eliminate overfitting, a useful way may be that we reduce the number of indices selected in step 1, when the sparsity s exceeds the critical sparsity. Therefore, we add some simple logic before iteration and modify STP as follows.

Algorithm 4 Subspace Thresholding Pursuit version 2

Input: $\mathbf{y}, \Phi, s, \alpha, \mu, \gamma$.

Initialization: $S^0 = \emptyset, \mathbf{x}^0 = \mathbf{0}$.

If $s > \gamma m$

then $\alpha s = \lceil 2\gamma m \rceil - s$.

else $\alpha s = s$.

Iteration: At the n -th iteration, go through the following steps.

- 1) $\Delta S = \{\alpha s \text{ indices corresponding to the } \alpha s \text{ largest magnitude entries in the vector } \Phi^* (\mathbf{y} - \Phi \mathbf{x}^{n-1})\}$.
- 2) $\tilde{S}^n = S^{n-1} \cup \Delta S$.
- 3) $\tilde{\mathbf{x}}^n = \arg \min_{\mathbf{z} \in \mathbb{R}^N} \{\|\mathbf{y} - \Phi \mathbf{z}\|_2, \text{supp}(\mathbf{z}) \subseteq \tilde{S}^n\}$.
- 4) $U^n = \{s \text{ indices corresponding to the } s \text{ largest magnitude elements of } \tilde{\mathbf{x}}^n\}$.
- 5) $\mathbf{u}^n = \{\text{the vector from } \tilde{\mathbf{x}}^n \text{ that keeps the entries of } \tilde{\mathbf{x}}^n \text{ in } U^n \text{ and set all other ones to zero.}\}$
- 6) $S^n = \{s \text{ indices corresponding to the } s \text{ largest magnitude entries of } \mathbf{u}^n + \mu \Phi^* (\mathbf{y} - \Phi \mathbf{u}^n)\}$.
- 7) $\mathbf{x}^n = \arg \min_{\mathbf{z} \in \mathbb{R}^N} \{\|\mathbf{y} - \Phi \mathbf{z}\|_2, \text{supp}(\mathbf{z}) \subseteq S^n\}$.

until the stopping criteria is met.

Output: $\mathbf{x}^n, \text{supp}(\mathbf{x}^n)$.

In the above modified version STPv2, we add a new parameter γ which is selected by user experience. Let s_* denote the critical sparsity of the corresponding STP algorithm in Gaussian signal case. Usually we select γ as $\frac{s_*}{m}$. By this modification, when s is larger than the critical sparsity of the corresponding STP algorithm, the cardinality of \tilde{S}^n will always be $\lceil 2\gamma m \rceil$, thus the overfitting problem is eliminated.

The two subfigures in Fig. 5 show the effect of this modification. In the two subfigures, we use the Gaussian measurement matrix of size 150×300 , 210×300 and perform 500 independent trails respectively. In each figure, we show the curve of STP and STPv2 both with optimal μ . In Fig. 5(a), the reconstruction capability of STPv2 starts to exceed the thresholding $\lceil m/2 \rceil$ which is the bottleneck of all iterative greedy algorithms that needs to keep a support set with size being equal or greater than $2s$ for solving a least-squares problems, such as SP, CoSaMP, STP. In Fig. 5(b), STPv2 exceeds STP greatly and the critical sparsity of STPv2 exceeds $\lceil m/2 \rceil$ a lot.

The modification has little impact on the reconstruction capability in CARS signal case since unless τ is too large, the reconstruction capability of STP will attain its limit before occuring overfitting; in addition, we select γ as $\frac{s_*}{m}$, because the critical sparsity in CARS signal case is smaller than that in Gaussian signal case, the reconstruction capability in CARS signal case will not be impacted naturally.

B. The improvement of other greedy algorithms by IHT-like identification

We can modify CoSaMP, HTP, SAMP and FBP by adding the IHT-like identification step in suitable step and denote the resulting algorithms as CoSaMPv2, HTPv2, SAMPv2 and FBPv2 respectively. As we

say in Section I, CoSaMP and HTP are representatives of iterative greedy algorithms, while SAMP and FBP can be treated as two different kinds of sparsity adaptive versions of SP, which are suitable to the situation that the sparsity s is unknown.¹ The main steps of the modified versions CoSaMPv2, HTPv2, SAMPv2 and FBPv2 are summarized in Alg. 5, 6, 7 and 8 respectively.

Algorithm 5 Compressive sampling matching pursuit version 2

Input: $\mathbf{y}, \Phi, s, \alpha, \mu$.

Initialization: $S^0 = \emptyset, \mathbf{x}^0 = \mathbf{0}$.

Iteration: At the n -th iteration, go through the following steps.

- 1) $\Delta S = \{\alpha s \text{ indices corresponding to the } \alpha s \text{ largest magnitude entries in the vector } \Phi^* (\mathbf{y} - \Phi \mathbf{x}^{n-1})\}$.
- 2) $\tilde{S}^n = S^{n-1} \cup \Delta S$.
- 3) $\tilde{\mathbf{x}}^n = \arg \min_{\mathbf{z} \in \mathbb{R}^N} \{\|\mathbf{y} - \Phi \mathbf{z}\|_2, \text{supp}(\mathbf{z}) \subseteq \tilde{S}^n\}$.
- 4) $U^n = \{s \text{ indices corresponding to the } s \text{ largest magnitude elements of } \tilde{\mathbf{x}}^n\}$.
- 5) $\mathbf{u}^n = \{\text{the vector from } \tilde{\mathbf{x}}^n \text{ that keeps the entries of } \tilde{\mathbf{x}}^n \text{ in } U^n \text{ and set all other ones to zero.}\}$
- 6) $\mathbf{x}^n = \{\text{the vector that keeps the } s \text{ largest magnitude entries of } \mathbf{u}^n + \mu \Phi^* (\mathbf{y} - \Phi \mathbf{u}^n) \text{ and set all other ones to zero.}\}$

until the stopping criteria is met.

Output: $\mathbf{x}^n, \text{supp}(\mathbf{x}^n)$.

Algorithm 6 Hard Thresholding Pursuit version 2

Input: $\mathbf{y}, \Phi, s, \alpha, \mu_1, \mu_2$.

Initialization: $S^0 = \emptyset, \mathbf{x}^0 = \mathbf{0}$.

Iteration: At the n -th iteration, go through the following steps.

- 1) $\tilde{S}^n = \{(\alpha + 1)s \text{ indices corresponding to the } (\alpha + 1)s \text{ largest magnitude entries in the vector } \mathbf{x}^{n-1} + \mu' \Phi^* (\mathbf{y} - \Phi \mathbf{x}^{n-1})\}$.
- 2) $\tilde{\mathbf{x}}^n = \arg \min_{\mathbf{z} \in \mathbb{R}^N} \{\|\mathbf{y} - \Phi \mathbf{z}\|_2, \text{supp}(\mathbf{z}) \subseteq \tilde{S}^n\}$.
- 3) $U^n = \{s \text{ indices corresponding to the } s \text{ largest magnitude elements of } \tilde{\mathbf{x}}^n\}$.
- 4) $\mathbf{u}^n = \{\text{the vector from } \tilde{\mathbf{x}}^n \text{ that keeps the entries of } \tilde{\mathbf{x}}^n \text{ in } U^n \text{ and set all other ones to zero.}\}$
- 5) $S^n = \{s \text{ indices corresponding to the } s \text{ largest magnitude entries of } \mathbf{u}^n + \mu \Phi^* (\mathbf{y} - \Phi \mathbf{u}^n)\}$.
- 6) $\mathbf{x}^n = \arg \min_{\mathbf{z} \in \mathbb{R}^N} \{\|\mathbf{y} - \Phi \mathbf{z}\|_2, \text{supp}(\mathbf{z}) \subseteq S^n\}$.

until the stopping criteria is met.

Output: $\mathbf{x}^n, \text{supp}(\mathbf{x}^n)$.

¹These algorithms don't need the sparsity s as their parameters, it is useful, but we should notice that if what we need is to reconstruct exact s -sparsity signals in noiseless environment with probability 1, because the critical sparsity can be tested a priori, so the demand of the parameter s has no limitation in this exact reconstruction situation if we use critical sparsity as the parameter s .

Algorithm 7 Sparsity Adaptive Matching Pursuit version 2

Input: $\mathbf{y}, \Phi, \text{init_size}, \mu$.

Initialization: $S^0 = \emptyset, \mathbf{x}^0 = \mathbf{0}, \nu = \text{init_size}$.

Iteration: At the n -th iteration, go through the following steps.

- 1) $\Delta S = \{\nu \text{ indices corresponding to the } \nu \text{ largest magnitude entries in the vector } \Phi^*(\mathbf{y} - \Phi \mathbf{x}^{n-1})\}$.
- 2) $\tilde{S}^n = S^{n-1} \cup \Delta S$.
- 3) $\tilde{\mathbf{x}}^n = \arg \min_{\mathbf{z} \in \mathbb{R}^N} \{\|\mathbf{y} - \Phi \mathbf{z}\|_2, \text{supp}(\mathbf{z}) \subseteq \tilde{S}^n\}$.
- 4) $U^n = \{s \text{ indices corresponding to the } s \text{ largest magnitude elements of } \tilde{\mathbf{x}}^n\}$.
- 5) $\mathbf{u}^n = \{\text{the vector from } \tilde{\mathbf{x}}^n \text{ that keeps the entries of } \tilde{\mathbf{x}}^n \text{ in } U^n \text{ and set all other ones to zero.}\}$
- 6) $V = \{s \text{ indices corresponding to the } s \text{ largest magnitude entries of } \mathbf{u}^n + \mu \Phi^*(\mathbf{y} - \Phi \mathbf{u}^n)\}$.
- 7) $\mathbf{v} = \arg \min_{\mathbf{z} \in \mathbb{R}^N} \{\|\mathbf{y} - \Phi \mathbf{z}\|_2, \text{supp}(\mathbf{z}) \subseteq V\}$.
 if the stopping criteria true then
 quit the iteration;
 elseif $\|\mathbf{y} - \Phi \mathbf{v}\|_2 \geq \|\mathbf{y} - \Phi \mathbf{x}^{n-1}\|_2$ then
 $\nu = \nu + \text{init_size}$;
 else
 $S^n = V$;
 $\mathbf{x}^n = \mathbf{v}$;
 end if

Output: $\mathbf{x}^n, \text{supp}(\mathbf{x}^n)$.

Algorithm 8 Forward backward Pursuit version 2

Input: $\mathbf{y}, \Phi, \mu, \nu, \chi$.

Initialization: $S^0 = \emptyset, \mathbf{x}^0 = \mathbf{0}$.

Iteration: At the n -th iteration, go through the following steps.

- 1) $\Delta S = \{\nu \text{ indices corresponding to the } \nu \text{ largest magnitude entries in the vector } \Phi^*(\mathbf{y} - \Phi \mathbf{x}^{n-1})\}$.
- 2) $\tilde{S}^n = S^{n-1} \cup \Delta S$.
- 3) $\tilde{\mathbf{x}}^n = \arg \min_{\mathbf{z} \in \mathbb{R}^N} \{\|\mathbf{y} - \Phi \mathbf{z}\|_2, \text{supp}(\mathbf{z}) \subseteq \tilde{S}^n\}$.
- 4) $U^n = \{s \text{ indices corresponding to the } s \text{ largest magnitude elements of } \tilde{\mathbf{x}}^n\}$.
- 5) $\mathbf{u}^n = \{\text{the vector from } \tilde{\mathbf{x}}^n \text{ that keeps the entries of } \tilde{\mathbf{x}}^n \text{ in } U^n \text{ and set all other ones to zero.}\}$
- 6) $S^n = \{|U^n| - \chi \text{ indices corresponding to the } |U^n| - \chi \text{ largest magnitude entries of } \mathbf{u}^n + \mu \Phi^*(\mathbf{y} - \Phi \mathbf{u}^n)\}$.
- 7) $\mathbf{x}^n = \arg \min_{\mathbf{z} \in \mathbb{R}^N} \{\|\mathbf{y} - \Phi \mathbf{z}\|_2, \text{supp}(\mathbf{z}) \subseteq S^n\}$.

until the stopping criteria is met.

Output: $\mathbf{x}^n, \text{supp}(\mathbf{x}^n)$.

The detailed descriptions of the original algorithms can be seen in [9], [13], [14], [17]. In the following paragraph, we only give the descriptions of the changes in CoSaMPv2, HTPv2, SAMPv2 and FBPv2 compared with the original algorithms as well as the settings in our simulations.

In our simulations, we use 100×1000 Gaussian measurement matrix and perform 500 independent trials respectively and give the algorithm descriptions of the four modifications as follows. In CoSaMPv2, we add the IHT-like identification step in step 6 and set $\alpha = 2$ in our simulations to imitate the initial version of CoSaMP in [9] (the more general description of CoSaMP can be seen in [27]); In HTPv2,

there exist two parameters μ' and μ which can be adjusted and both two identification steps in steps 1 and 5 are IHT-like identification steps. Let $|\mathbf{v}|_{\min}, |\mathbf{v}|_{\max}$ denote the smallest magnitude entries and the largest entries in arbitrary vector \mathbf{v} , due to $(\Phi^*(\mathbf{y} - \Phi\mathbf{x}^{n-1}))_{S^{n-1}} = \mathbf{0}$, when $\mu' < \frac{|\mathbf{x}^{n-1}|_{\min}}{|\Phi^*(\mathbf{y} - \Phi\mathbf{x}^{n-1})|_{\max}}$, in step 1 of HTPv2, \tilde{S}^n will contain $\text{supp}(\mathbf{x}^{n-1})$ first, then HTPv2 degrades to STP. In addition, if we set $\alpha = 0, \mu' = \mu = 1$, HTPv2 degrades to HTP. In order to stand for general case, we set $\alpha = 1, \mu' = 1$ in our simulations. In SAMPv2, we add the IHT-like identification step in steps 5 and 6 and set $\text{init_size} = 2$ in our simulations; in FBPv2, we add the IHT-like identification steps 5 and 6 and set $\nu = 20, \chi = 18$.

The four subfigures in Fig. 6 and 7 show their empirical performance. We show the performance of CoSaMPv2 and HTP v2 in Fig. 6(a), 6(b) and then the performance of SAMPv2 and FBPv2 in Fig. 7(a), 7(b). In each figure, we display the curve of each algorithm with optimal μ if it needs the parameter μ . We show that IHT-like identification step is a universal way to improve the empirical performance, but so far, in all of these improvements, the improvement to SP, i.e., the proposed STP algorithm has better empirical performance than the other improvements.

VI. CONCLUSION

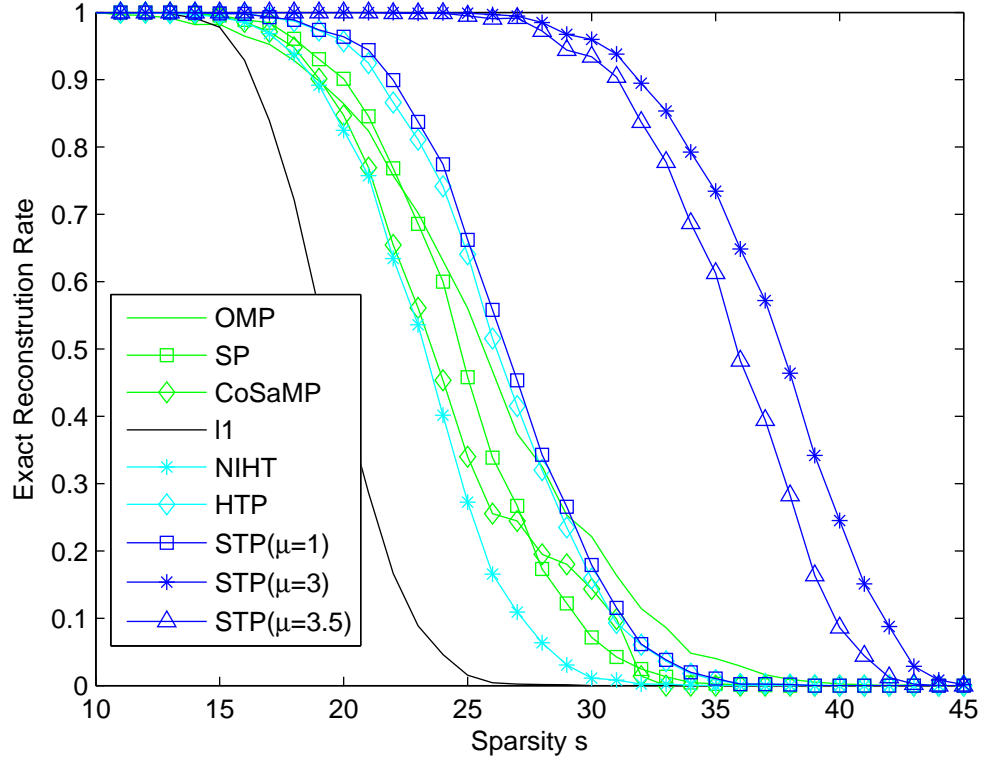
In this paper, we proposed a new reconstruction algorithm for CS, termed subspace thresholding pursuit (STP). STP has strong provable theoretical guarantee and excellent empirical performance. It digs out the potential of iterative greedy algorithms further and displays an outstanding worst-case empirical performance which is better than the well-known ℓ_1 minimization in practical situation. Generally, there is no tradeoff between reconstruction performance and computational complexity when we use STP instead of the existing iterative greedy algorithms in practice. In addition, we observed the overfitting problem and proposed a simple but effective way to eliminate it and showed the universal significance of the idea in STP. Future works may focus on solving the inconsistency of the theoretical guarantee and empirical performance of the paper, e.g., STP with some parameter $\mu > 1$ may have better empirical performance but worse theoretical guarantee than the one with $\mu = 1$ in the current version.

ACKNOWLEDGEMENT

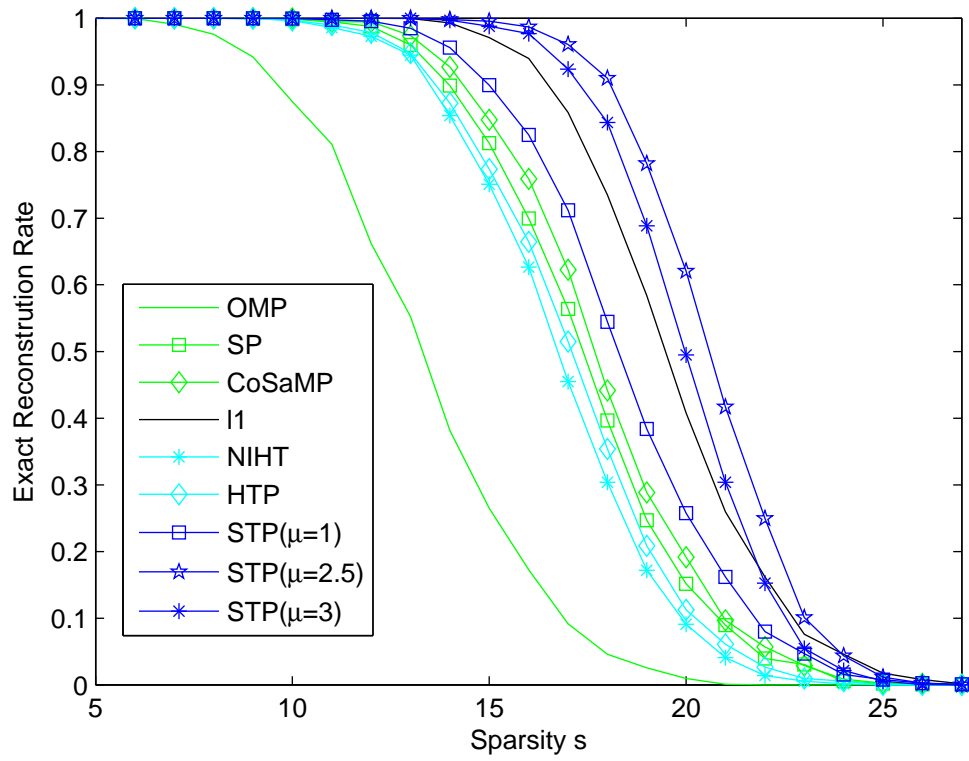
The authors would like to thank Mr. Xin-Ji Liu for the valuable suggestions that improved the presentation of the paper.

REFERENCES

- [1] D. L. Donoho, "Compressed sensing," *IEEE Transactions on Information Theory*, vol. 52, no. 4, pp. 1289–1306, 2006.
- [2] E. J. Candès and T. Tao, "Decoding by linear programming," *IEEE Transactions on Information Theory*, vol. 51, no. 12, pp. 4203–4215, 2005.
- [3] E. J. Candès, J. Romberg, and T. Tao, "Robust uncertainty principles: Exact signal reconstruction from highly incomplete frequency information," *IEEE Transactions on Information Theory*, vol. 52, no. 2, pp. 489–509, 2006.
- [4] D. L. Donoho and M. Elad, "Optimally sparse representation in general (nonorthogonal) dictionaries via ℓ_1 minimization," *Proceedings of the National Academy of Sciences*, vol. 100, no. 5, pp. 2197–2202, 2003.
- [5] S. Jafarpour, W. Xu, B. Hassibi, and R. Calderbank, "Efficient and robust compressed sensing using optimized expander graphs," *IEEE Transactions on Information Theory*, vol. 55, no. 9, pp. 4299–4308, 2009.
- [6] D. Baron, S. Sarvotham, and R. G. Baraniuk, "Bayesian compressive sensing via belief propagation," *IEEE Transactions on Signal Processing*, vol. 58, no. 1, pp. 269–280, 2010.
- [7] Y. C. Pati, R. Rezaifar, and P. Krishnaprasad, "Orthogonal matching pursuit: Recursive function approximation with applications to wavelet decomposition," in *Signals, Systems and Computers, 1993. 1993 Conference Record of The Twenty-Seventh Asilomar Conference on*. IEEE, 1993, pp. 40–44.
- [8] D. Needell and R. Vershynin, "Signal recovery from incomplete and inaccurate measurements via regularized orthogonal matching pursuit," *Selected Topics in Signal Processing, IEEE Journal of*, vol. 4, no. 2, pp. 310–316, 2010.
- [9] D. Needell and J. A. Tropp, "CoSaMP: Iterative signal recovery from incomplete and inaccurate samples," *Applied and Computational Harmonic Analysis*, vol. 26, no. 3, pp. 301–321, 2009.
- [10] W. Dai and O. Milenkovic, "Subspace pursuit for compressive sensing signal reconstruction," *IEEE Transactions on Information Theory*, vol. 55, no. 5, pp. 2230–2249, 2009.
- [11] B. Shim, J. Wang, and S. Kwon, "Generalized orthogonal matching pursuit," *IEEE Transactions on Signal Processing*, vol. 60, pp. 6202–6216, 2012.
- [12] E. Liu and V. N. Temlyakov, "The orthogonal super greedy algorithm and applications in compressed sensing," *IEEE Transactions on Information Theory*, vol. 58, no. 4, pp. 2040–2047, 2012.
- [13] T. T. Do, L. Gan, N. Nguyen, and T. D. Tran, "Sparsity adaptive matching pursuit algorithm for practical compressed sensing," in *2008 42nd Asilomar Conference on Signals, Systems and Computers*. IEEE, 2008, pp. 581–587.
- [14] N. B. Karahanoglu and H. Erdogan, "Compressed sensing signal recovery via forward-backward pursuit," *Digital Signal Processing*, 2013.
- [15] T. Blumensath and M. E. Davies, "Iterative hard thresholding for compressed sensing," *Applied and Computational Harmonic Analysis*, vol. 27, no. 3, pp. 265–274, 2009.
- [16] R. Garg and R. Khandekar, "Gradient descent with sparsification: an iterative algorithm for sparse recovery with restricted isometry property," in *Proceedings of the 26th Annual International Conference on Machine Learning*. ACM, 2009, pp. 337–344.
- [17] S. Foucart, "Hard thresholding pursuit: an algorithm for compressive sensing," *SIAM Journal on Numerical Analysis*, vol. 49, no. 6, pp. 2543–2563, 2011.
- [18] T. Blumensath and M. E. Davies, "Normalized iterative hard thresholding: Guaranteed stability and performance," *IEEE Journal of Selected Topics in Signal Processing*, vol. 4, no. 2, pp. 298–309, 2010.
- [19] Q. Mo and Y. Shen, "A remark on the restricted isometry property in orthogonal matching pursuit," *IEEE Transactions on Information Theory*, vol. 58, no. 6, pp. 3654–3656, 2012.
- [20] J. Wang and B. Shim, "On the recovery limit of sparse signals using orthogonal matching pursuit," *Signal Processing, IEEE Transactions on*, vol. 60, no. 9, pp. 4973–4976, 2012.
- [21] C.-B. Song, S.-T. Xia, and X.-j. Liu, "Improved Analyses for SP and CoSaMP Algorithms in Terms of Restricted Isometry Constants," *arXiv preprint arXiv:1309.6073*, 2013.
- [22] J. D. Blanchard, M. Cermak, D. Hanle, and Y. Jing, "Greedy algorithms for joint sparse recovery." [Online]. Available: <http://www.math.grin.edu/~blanchaj/Research/GAJS.pdf>
- [23] A. Maleki and D. L. Donoho, "Optimally tuned iterative reconstruction algorithms for compressed sensing," *IEEE Journal of Selected Topics in Signal Processing*, vol. 4, no. 2, pp. 330–341, 2010.
- [24] J. D. Blanchard, C. Cartis, J. Tanner, and A. Thompson, "Phase transitions for greedy sparse approximation algorithms," *Applied and Computational Harmonic Analysis*, vol. 30, no. 2, pp. 188–203, 2011.
- [25] E. Candès, M. Rudelson, T. Tao, and R. Vershynin, "Error correction via linear programming," in *Foundations of Computer Science, 2005. FOCS 2005. 46th Annual IEEE Symposium on*. IEEE, 2005, pp. 668–681.
- [26] M. E. Davies, R. Gribonval *et al.*, "Restricted isometry constants where ℓ_p sparse recovery can fail for $0 < p \leq 1$," *IEEE Transactions on Information Theory*, vol. 55, no. 5, pp. 2203–2214, 2009.
- [27] J. A. Tropp and S. J. Wright, "Computational methods for sparse solution of linear inverse problems," *Proceedings of the IEEE*, vol. 98, no. 6, pp. 948–958, 2010.

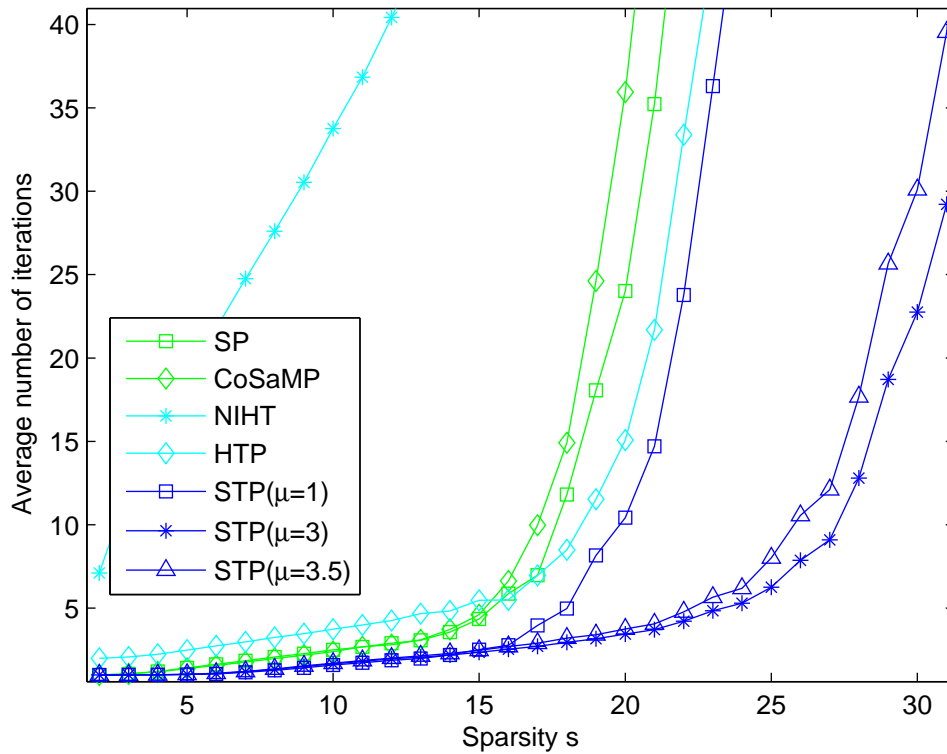


(a) Exact reconstruction rate in Gaussian signal case

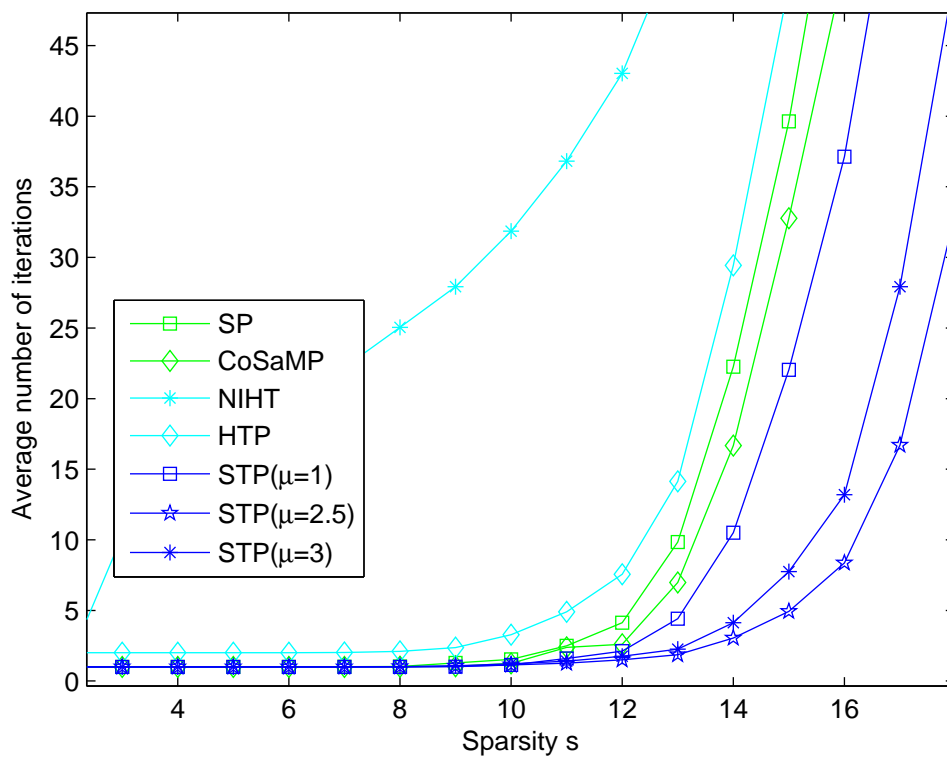


(b) Exact reconstruction rate in CARS signal case

Figure 2. Exact reconstruction rate under 100×1000 Gaussian measurement matrix with $\tau = 0.1$.

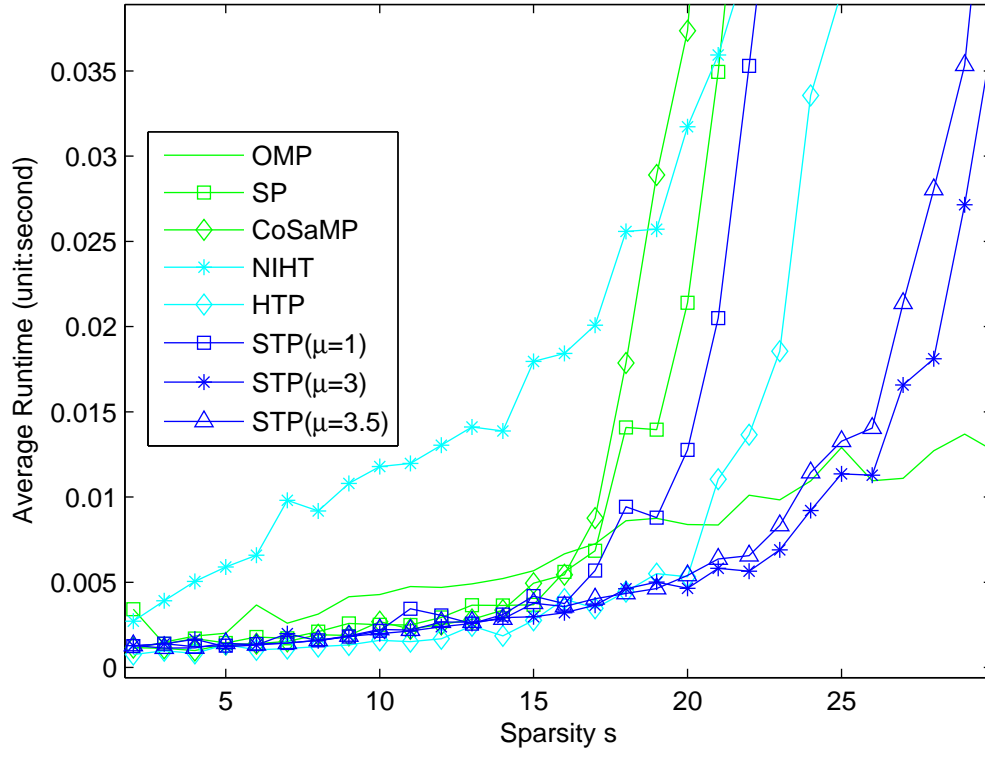


(a) Average Number of iterations in Gaussian signal case

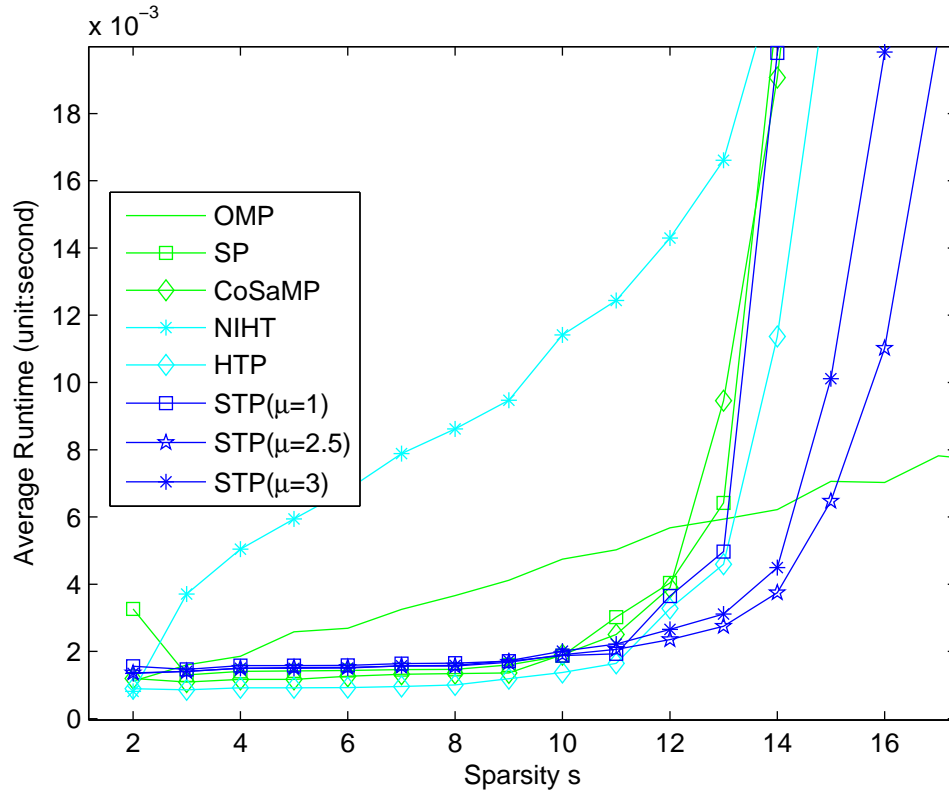


(b) Average Number of iterations in CARS signal case

Figure 3. Average Number of iterations under 100×1000 Gaussian measurement matrix with $\tau = 0.1$.



(a) Average Runtime in CARS signal case



(b) Average Runtime in CARS signal case

Figure 4. Average Runtime under 100×1000 Gaussian measurement matrix with $\tau = 0.1$.

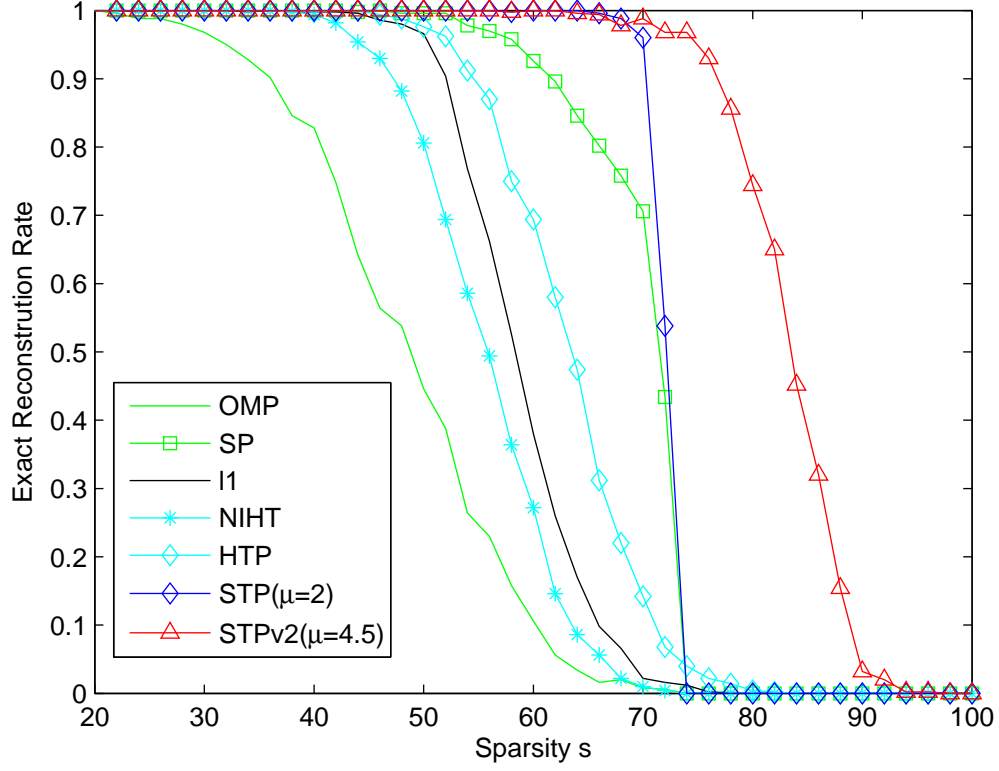
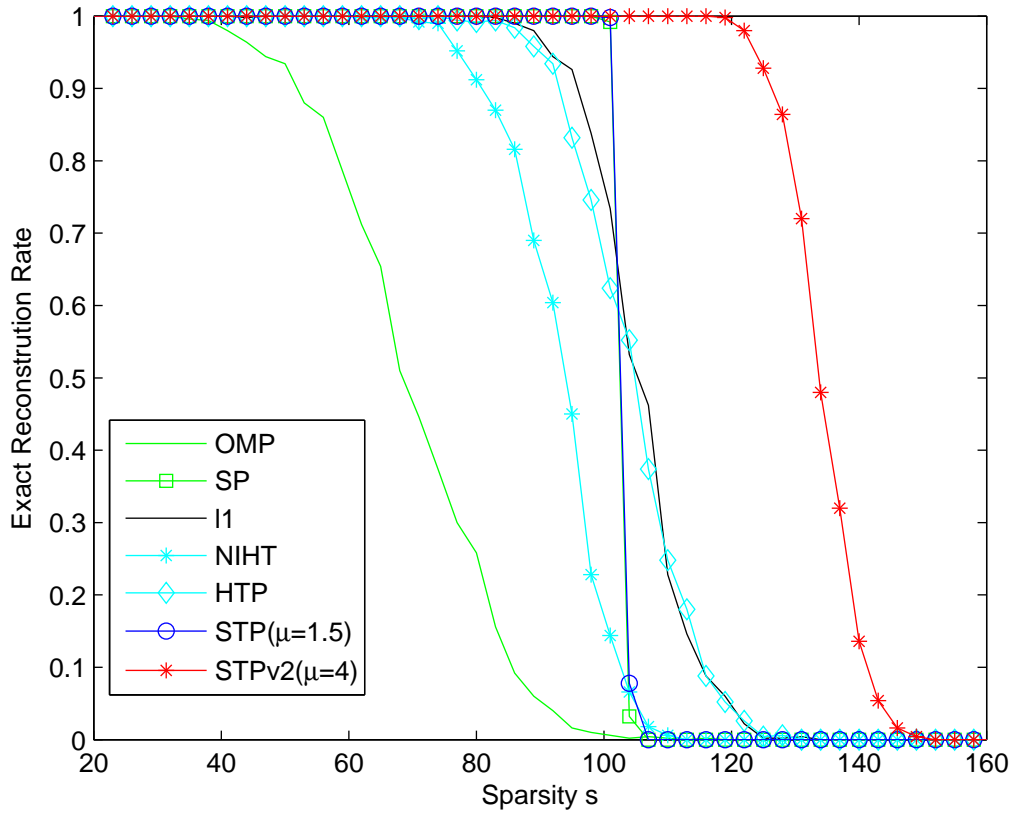
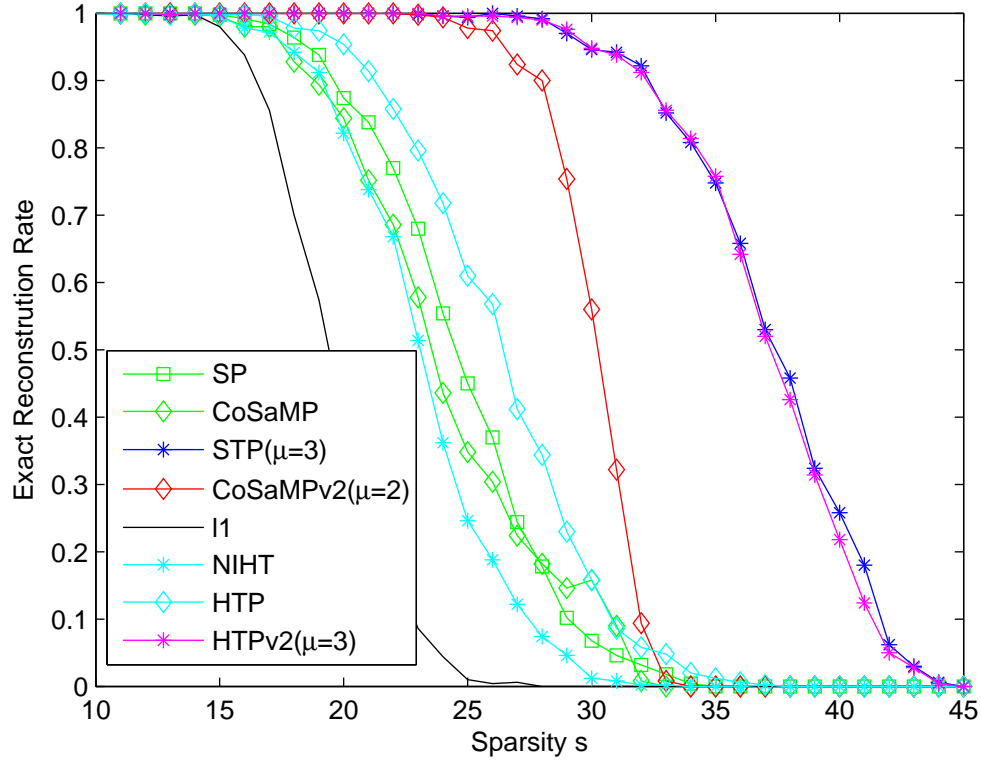
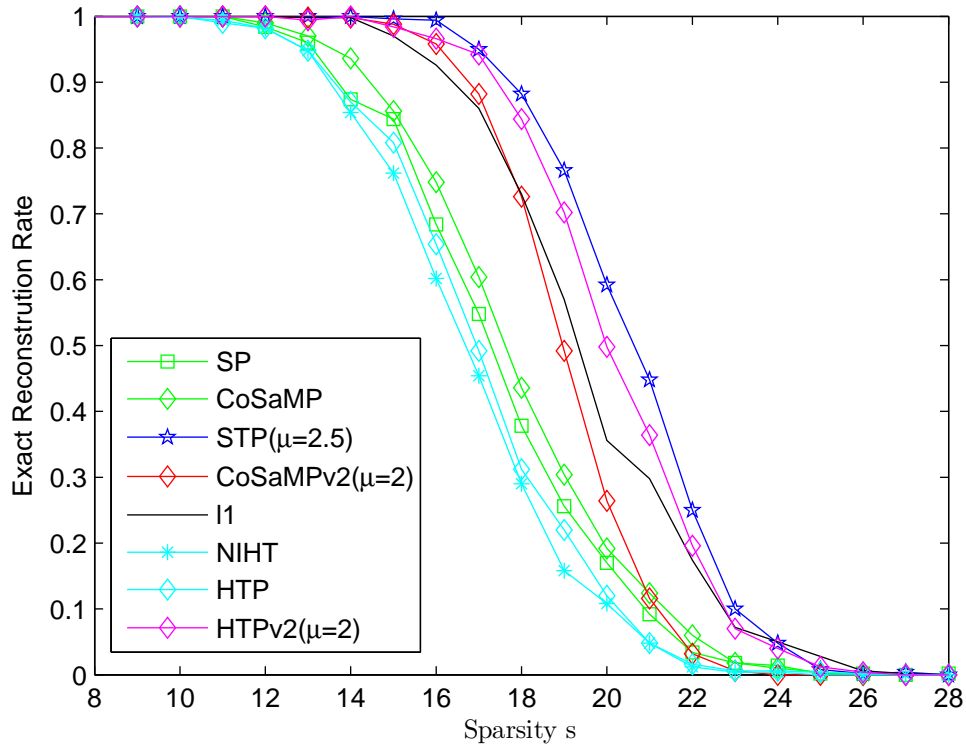
(a) Exact reconstruction rate under 150×300 Gaussian measurement matrix(b) Exact reconstruction rate under 210×300 Gaussian measurement matrix

Figure 5. The performance test of STPv2 in Gaussian signal case.

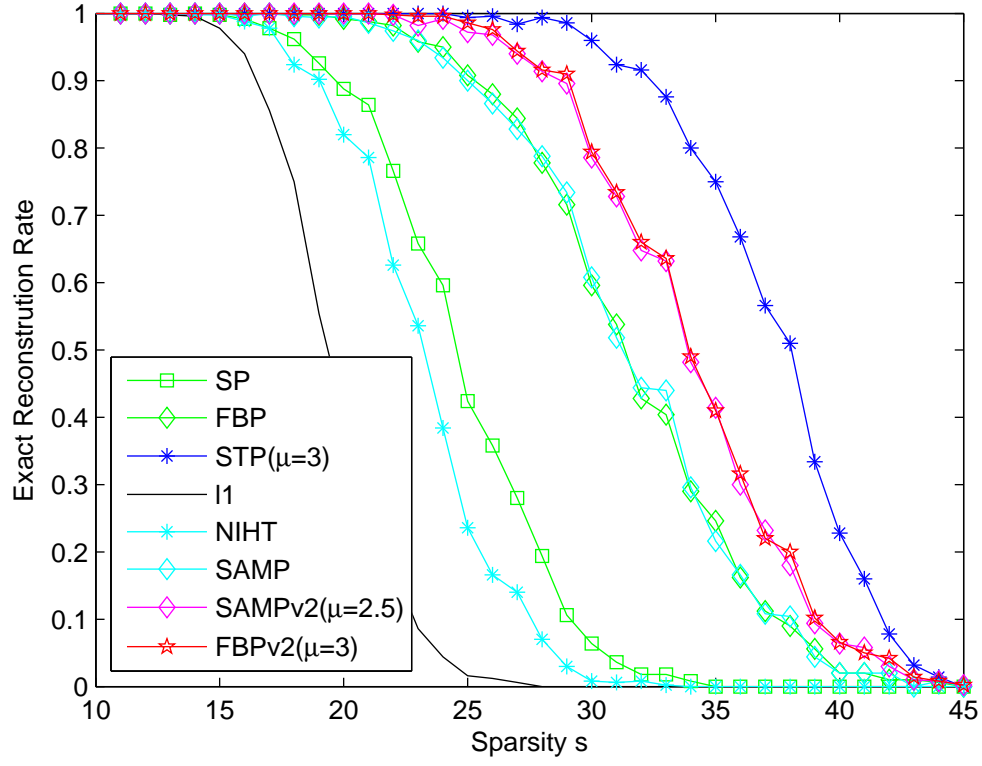


(a) Exact reconstruction rate of CoSaMPv2 and HTPv2 in Gaussian signal case

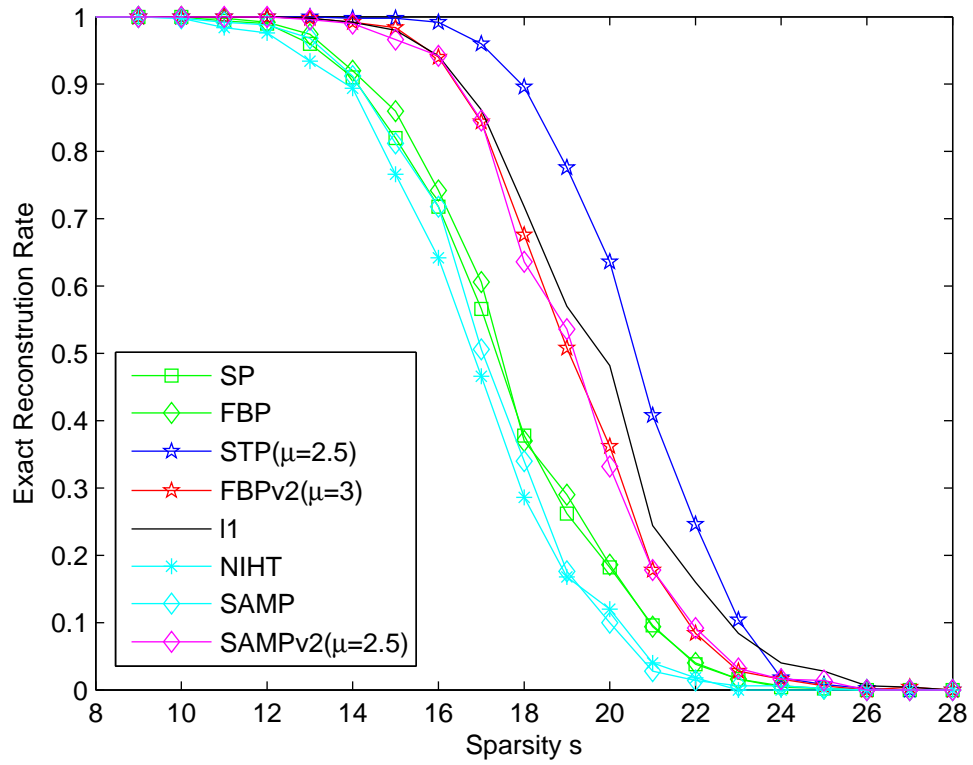


(b) Exact reconstruction rate of CoSaMPv2 and HTPv2 in CARS signal case

Figure 6. The performance test of CoSaMPv2 and HTPv2 under 100×1000 Gaussian measurement matrix with undersampling ratio $\tau = 0.1$.



(a) Exact reconstruction rate of SAMPv2 and FBPv2 in Gaussian signal case



(b) Exact reconstruction rate of SAMPv2 and FBPv2 in CARS signal case

Figure 7. The performance test of SAMPv2 and FBPv2 under 100×1000 Gaussian measurement matrix with undersampling ratio $\tau = 0.1$.